THE ASTROPHYSICAL JOURNAL, 309:804–821, 1986 October 15

MOLECULAR CLOUDS AND SUPERNOVA REMNANTS IN THE OUTER GALAXY

Y.-L. HUANG[1] AND P. THADDEUS
Goddard Institute for Space Studies; and Department of Physics, Columbia University
Received 1985 October 30; accepted 1986 April 7

ABSTRACT

The study of extragalactic supernovae (SNs) suggests that Type II SNs, not Type I, tend to occur near extreme optical Population I objects (e.g., OB associations or giant H II regions), but the detection of these objects in our Galaxy is limited by heavy local obscuration. Large molecular clouds, which occur near most OB associations or giant H II regions and can be detected up to great distances, are the most easily used objects for studying the environment of SNs and identifying remnants of Galactic Type II SNs. We carried out a CO survey toward every confirmed outer Galaxy supernova remnant (SNR) from $l = 70°$–$210°$, for a total of 26, and found that roughly half of them, within uncertainties of distance estimates, revealed spatial coincidences with large molecular cloud complexes. Most of the cloud complexes in these coincidences probably are the birthplaces of the progenitors of the corresponding Type II SNRs, because it is statistically improbable that the coincidences result from chance superposition.

Subject headings: interstellar: molecules — nebulae: supernova remnants

I. INTRODUCTION

Nearly 600 extragalactic supernovae (SNs) have been observed, but where they originate and what kind of progenitor stars they result from remain quite unclear. Even though the supernova remnants (SNRs) in our Galaxy are relatively old, studying their environments may help us to answer these questions because they are so close.

Examining the locations of extragalactic SNs from optical photos provides some information about the environment of SNs (Maza and van den Bergh 1976; Huang 1985): Type II events, but not Type I, in spiral galaxies tend to occur near nebulous knots, objects shown from Hα surveys to be OB associations, or giant H II regions located in spiral arms. If our Galaxy is a typical Sc galaxy (Hodge 1983), where the ratio for the occurrence of Type I to Type II SNs is, within statistical error, on the order of one, we may expect roughly half the Galactic SNRs, viz. those from Type II events, to occur near OB associations or giant H II regions. Several investigations (Akhundova, Guseinov, and Rakhamimov 1975; Montmerle 1979; Allakhverdiyev *et al.* 1983) attempted to establish a connection between SNRs and OB associations based on positional coincidence, but because heavy local obscuration limited detection of OB associations in the Galaxy, these studies were seriously biased against distant remnants and were inconclusive. Large molecular clouds may be the best objects with which to study the environment of SNs in detail, because they are the placental clouds of OB associations and giant H II regions and are easily detected with the trace molecule CO throughout the Galaxy (e.g., Dame and Thaddeus 1985).

Estimating distance is crucial in the study of the relation between an SNR and a molecular cloud. Most attempts to measure the distances of Galactic SNRs have been based on kinetics of H I absorption features or Hα filaments, but generally such attempts can provide only uncertain estimates (Allakhverdiyev *et al.* 1983; Green 1984). The empirical Σ-D relation (see, e.g., Caswell and Lerche 1979; Milne 1979) has often served to estimate the distances, even though it shows large scatter; we have used the Σ-D relation of Milne (1979), the one without correction for the questionable $|z|$-effect (see Huang and Thaddeus 1985 for details), which provides an uncertainty of a factor of 2 for the distances estimated (see Milne's Fig. 1*b*).

The distance to a molecular cloud may be obtained from the spectrophotometric distance of an accompanying OB association, which is little biased by the inaccuracies in the distance estimates of individual member stars and allows an uncertainty of roughly $\pm 15\%$. Should no OB association appear in or near the cloud, the spectrophotometric distance (with an uncertainty of $\sim \pm 25\%$ based on only a few exciting stars) of an accompanying H II region serves. The kinematic distance of the cloud beyond the solar circle, for which we adopted a flat rotation curve ($V_\odot = 250$ km s^{-1} and $R_\odot = 10$ kpc) that offers a good compromise among curves previously derived (e.g., Schmidt 1965; Blitz, Fich, and Stark 1980; Clemens 1985), is used if no spectrophotometric distance is available, although it usually gives a larger uncertainty (say, $\pm 35\%$); large noncircular motions, for example, are observed in the area from $l = 100°$–$140°$ and near $l = 160°$ (Rickard 1968; Georgelin, Georgelin, and Roux 1973). The conclusion of our work will not be affected if $V_\odot = 220$ km s^{-1} and $R_\odot = 8.5$ kpc (Knapp, Tremaine, and Gunn 1978) are chosen.

Only a few CO observations (e.g., Cornett 1977; Wootten 1978; Scoville *et al.* 1977), intended mainly to search for evidence of SNR–cloud interaction, were available toward SNRs, most of them on a small scale and seriously undersampled. In this paper we present a large-scale, well-sampled CO survey near 26 northern SNRs. The CO observations, which provide information on molecular gas content, combined with observations at other frequencies, provide a much cleaner picture than previously available of the environment of SNs. In § II we describe the observations, and in § III we present our CO data and discuss individual SNRs. Section IV gives a statistical study of the apparent coincidences between SNRs and large molecular clouds, and, last, in § V our results are summarized and our conclusions given.

[1] Also Five College Radio Astronomy Observatory, University of Massachusetts.

II. OBSERVATIONS

With its moderate angular resolution ($\sim 8'.7$) and high sensitivity, the GISS–Columbia 1.2 m telescope is one of the best existing instruments for a systematic CO ($1 \rightarrow 0$) search for molecular clouds near SNRs. During the period of the present survey, carried out from 1981 to 1984, a major improvement to the receiver was made: in the summer of 1983, the room-temperature, double-sideband Schottky mixer was replaced by a liquid helium–cooled, single-sideband SIS mixer (Pan *et al.* 1983) which reduced the single-sideband receiver noise temperature from 840 to 90 K. This nearly order-of-magnitude improvement made sky noise and spillover, rather than receiver noise, the dominant contribution to the system noise. The low noise of the SIS receiver shortened the integration time of our observations by a factor of 10–20, depending on elevation.

We confined the search for accompanying molecular clouds to the outer Galaxy SNRs that lie within the longitude range 70°–210°. Twenty-nine confirmed SNRs of a total of roughly 140 in the Galaxy (see, e.g., van den Bergh 1983) are located in this range and three of these (the Cygnus Loop, γ Cygni SNR, and W63) lie within the solar circle. Our sample (Table 1) therefore consists of 26 SNRs. This selection provides two advantages:

1. No longitude or velocity crowding is expected, because the location of the solar system in the Galaxy allows the survey to cover a relatively small portion of the Galactic disk but span a large longitude range where large molecular clouds are relatively sparse (unlike the dense concentration in the inner Galaxy).
2. No ambiguity in kinematic distances exists for outer Galaxy clouds.

To allow for the possible migration of the progenitor star of an SNR away from the molecular cloud where it formed, we first mapped coarsely a much larger area than the face of each remnant—typically larger than a $1^\circ \times 1^\circ$ area—then sampled thoroughly any cloud for which the distance agrees, within uncertainties, with the distance of the SNR. For four SNRs (Simeiz 147, IC 443, G192.8 − 1.1, and the Monoceros Loop) in the third quadrant (owing to the limited observing time and their large angular sizes), we used data from an independent $0^\circ.5$ resolution CO survey that we carried out to study the distribution of clouds in the outer Galaxy and fully covered an area from $l = 178^\circ$ to 210°, $b = -6^\circ$ to $+5^\circ$. The $0^\circ.5$ resolution was obtained synthetically by scanning a 4×4 raster of points separated by $\frac{1}{8}^\circ$ (roughly the beamwidth of the telescope) and summing the resultant 16 spectra.

Position switching was used for all our observations to ensure flat spectral baselines. The integration time for each observation, chosen to give an rms noise of ~ 0.3 K in the resultant spectrum, was typically 12 minutes with the Schottky receiver and 45 s with the SIS receiver. The spectrometer used is a filter bank of 256 channels, each 250 kHz wide, that provides a velocity resolution of 0.65 km s^{-1} at 115 GHz. The

TABLE 1

PARAMETERS OF OUTER GALAXY SUPERNOVA REMNANTS WITHIN $l = 70^\circ$–210°

Galactic Name Designation	Other Name	Angular Diameter	Spectral Index[a]	Surface Brightness (W m^{-2} Hz^{-1} sr^{-1}) 1 GHz	Surface Brightness (W m^{-2} Hz^{-1} sr^{-1}) 408 MHz	Distance[b] (kpc)	Diameter[b] (pc)	Reference
G74.9+1.2.....	CTB 87	7.4	−0.24	0.18E−19	0.23E−19	10.7	23.1	1
G84.2−0.8.....	...	18.0	−0.50	0.46E−20	0.72E−20	6.3	33.0	2
G89.0+4.7.....	HB 21	100.0	−0.40	0.39E−20	0.56E−20	1.2	34.4	3
G93.3+6.9.....	DA 530	23.2	−0.56	0.25E−20	0.41E−20	5.7	38.6	4
G93.7−0.3.....	CTB 104A	92.5	−0.34	0.11E−20	0.15E−20	1.8	47.8	5
G94.0+1.0.....	3C 434.1	30.0	−0.44	0.20E−20	0.28E−20	4.7	40.9	6
G109.2−1.0.....	CTB 109	29.4	−0.50	0.35E−20	0.55E−20	4.1	35.4	7
G111.7−2.1.....	Cas A	4.2	−0.76	0.29E−16	0.57E−16	2.8	3.4	8, 9
G114.3+0.3.....	...	97.0	−0.29	0.12E−21	0.16E−21	3.0	85.1	10
G116.5+1.1.....	...	73.0	−0.83	0.32E−21	0.67E−21	3.1	65.9	10
G116.9+0.2.....	CTB 1	35.5	−0.51	0.12E−20	0.17E−20	4.5	46.8	11
G119.5+9.8.....	CTA 1	107.0	−0.47	0.50E−21	0.72E−21	1.9	58.7	12
G120.1+1.4.....	Tycho's SNR	7.9	−0.55	0.14E−18	0.22E−18	5.9	13.6	13
G126.2+1.6.....	...	68.0	(−0.48)	0.23E−21	0.29E−21	3.6	71.8	14
G127.1+0.5.....	...	54.6	−0.60	0.65E−21	0.11E−20	3.5	54.8	15
G130.7+3.1.....	3C 58	7.7	−0.09	0.83E−19	0.91E−19	6.9	15.5	16
G132.7+1.3.....	HB 3	90.0	−0.52	0.20E−20	0.32E−20	1.6	40.9	8, 17
G160.4+2.8.....	HB 9	130.0	−0.58	0.11E−20	0.18E−20	1.3	47.8	18, 19
G166.1+4.4.....	VRO 42.05.01	49.0	(−0.40)	0.51E−21	0.69E−21	4.1	58.4	9, 20
G166.3+2.5.....	OA 184	76.0	(−0.59)	0.26E−21	0.44E−21	3.1	69.6	21,22
G180.3−1.7.....	Simeis 147	166.0	...	0.30E−21	0.55E−21	1.4	67.0	23, 24
G184.6−5.8.....	Crab Nebula	5.9	−0.26	0.44E−17	0.55E−17	3.2	5.5	16
G189.0+3.0.....	IC 443	40.0	−0.36	0.15E−19	0.21E−19	2.1	24.2	9, 25
G192.8−1.1.....	...	78.0	(−0.55)	0.48E−21	0.79E−21	2.6	59.3	26
G205.6−0.1.....	Mon Loop	247.0	−0.47	0.44E−21	0.67E−21	0.8	60.7	27
G206.9+2.3.....	PKS 0646+06	51.2	−0.45	0.37E−21	0.56E−21	4.3	63.5	27

[a] Values in parentheses are uncertain.

[b] Determined from the $|z|$-uncorrected Σ-D relation of Milne 1979.

REFERENCES.—(1) Weiler and Shaver 1978. (2) Matthews *et al.* 1977. (3) Willis 1973. (4) Haslam *et al.* 1980. (5) Mantovani *et al.* 1982. (6) Goss *et al.* 1984. (7) Hughes *et al.* 1984. (8) Clark and Caswell 1976. (9) Milne 1979. (10) Reich and Braunsfurth 1981. (11) Landecker *et al.* 1982. (12) Sieber *et al.* 1981. (13) Duin and Strom 1975. (14) Furst *et al.* 1984. (15) Salter *et al.* 1978. (16) Wilson and Weiler 1976. (17) Braunsfurth 1983. (18) Dwarakanath *et al.* 1982. (19) Reich 1983. (20) Landecker *et al.* 1982*a*. (21) Caswell and Lerche 1979. (22) Dickel and DeNoyer 1975. (23) Sofue *et al.* 1980. (24) Haslam and Salter 1971. (25) Erickson and Mahoney 1984. (26) Caswell 1985. (27) Graham *et al.* 1982.

telescope is calibrated with a standard room-temperature blackbody chopper wheel which automatically corrects for atmospheric attenuation; the line intensity given here has been corrected for beam efficiency according to the Rayleigh-Jeans formula to yield the radiation temperature $T_R = \lambda^2 I_\nu / 2k$, where I_ν is the radiation intensity. Observational information for each SNR, e.g., the sampling and the observing parameters, can be found in more detail in Huang (1985).

III. COMMENTS ON INDIVIDUAL SUPERNOVA REMNANTS

Our CO data toward each SNR are summarized in this section. The molecular distributions are generally presented as contour maps of velocity-integrated CO emission $W_{CO} = \int T_R \, dv$; contours enclosing depressions (down-going contours) are dotted. In many cases, the positions of the SNR and neighboring young optical objects are also shown in the maps; the SNRs are denoted by shaded regions, the H II regions and optical filaments of the SNRs by striated lines.

We here define a molecular cloud complex as a group of CO features close both on the plane of the sky and in radial velocity. Even though these smaller features do not always connect with each other they are probably interrelated, because the overall density of clouds (especially in the outer Galaxy) is far too low for these to be merely statistical fluctuations in the distribution of smaller clouds (see, e.g., Dame *et al.* 1986).

In order to estimate the masses of the detected cloud complexes, we assumed a proportionality between H_2 column density $N(H_2)$ and W_{CO}. For inner Galaxy clouds, a conversion factor of $N(H_2)/W_{CO} = 2 \pm 1 \times 10^{20}$ cm^{-2} K^{-1} km^{-1} s is recently calibrated by Lebrun *et al.* (1983), using γ-rays as a total gas tracer and the 21 cm emission as an atomic gas tracer. This conversion factor may have been underestimated for outer Galaxy clouds, because the cosmic-ray fluxes are expected to be higher in inner Galaxy clouds. For outer Galaxy clouds, we adopted a value of 2.6×10^{20} cm^{-2} K^{-1} km^{-1} s, the conversion factor derived for the Orion cloud complex (located near the solar circle) by Bloemen *et al.* (1984). Taking 2.72 for the mean molecular weight per H_2 (Allen 1973), the mass (in units of solar masses) of a molecular cloud complex can be expressed as

$$M = 1.7 \times 10^3 I_{CO} r^2 ,$$

where r (in kpc) is distance to the cloud complex and I_{CO} (in K km s^{-1} deg^2) is total CO luminosity, i.e., W_{CO} integrated over the face of the complex. In this paper, we define a cloud complex more massive than $10^5 M_\odot$ as a *large* molecular cloud complex.

G74.9+1.2 (CTB 87).—One of the few Crablike SNRs in the Galaxy, this SNR is suggested to lie no closer than a marginally revealed H I absorption feature at -77 km s^{-1}, based on observations carried out with a relatively large telescope beam (Kazes and Caswell 1977). An observation of high angular resolution and good spectral calibration may be needed to establish the distance to CTB 87.

Our CO observations show a cloud at -57 km s^{-1} (Fig. 1), in excellent agreement with the strongest H I absorption feature at -59 km s^{-1} (Kazes and Caswell 1977). Adopting a kinematic distance of 11.4 kpc, the cloud's mass was calculated to be $1.6 \times 10^5 M_\odot$. Since SNRs and large molecular clouds are both rare at such a large galactocentric distance (~ 13 kpc), an association between CTB 87 and the cloud is fairly certain; such an association is further supported by the fact that this cloud is the only site detected of massive-star formation in the vicinity, if, as Nomoto (1983) suggests, Crablike remnants originate from stars of 8–10 $M_\odot$.

G84.2−0.8.—This shell-like remnant has a Σ-D distance of 6.3 kpc (Table 1), placing it well beyond a prominent foreground dark cloud complex (see, e.g., Bally and Scoville 1980; Dame and Thaddeus 1985) associated with the North American and Pelican nebulae. Heavy local obscuration and the large distance hamper optical detection of young objects in its vicinity.

A molecular cloud complex with peak velocities from $V_{LSR} = -44$ to -33 km s^{-1}, corresponding to a kinematic distance of 6.7–7.8 kpc, was observed next to the remnant at a

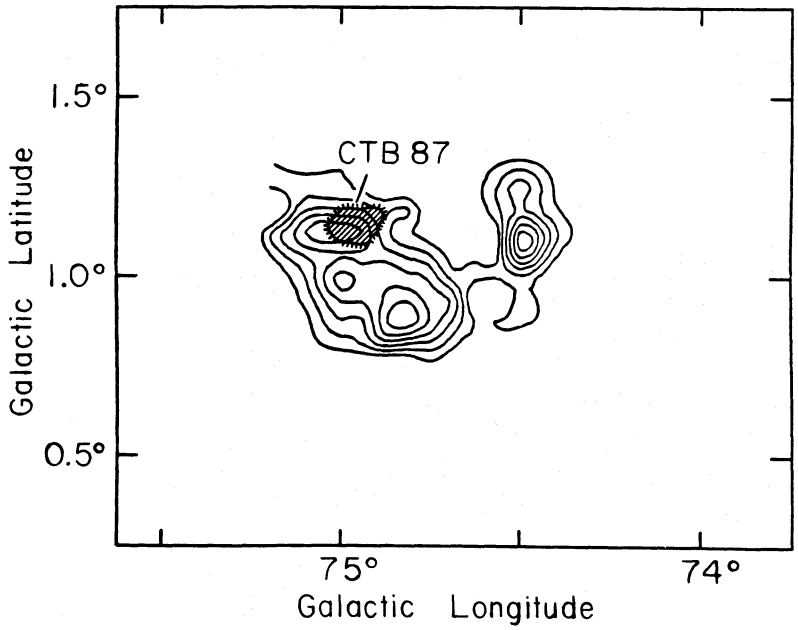

FIG. 1.—SNR CTB 87; map integrated over velocity from -63 to -53 km s^{-1} with a contour interval of 1 K km s^{-1}

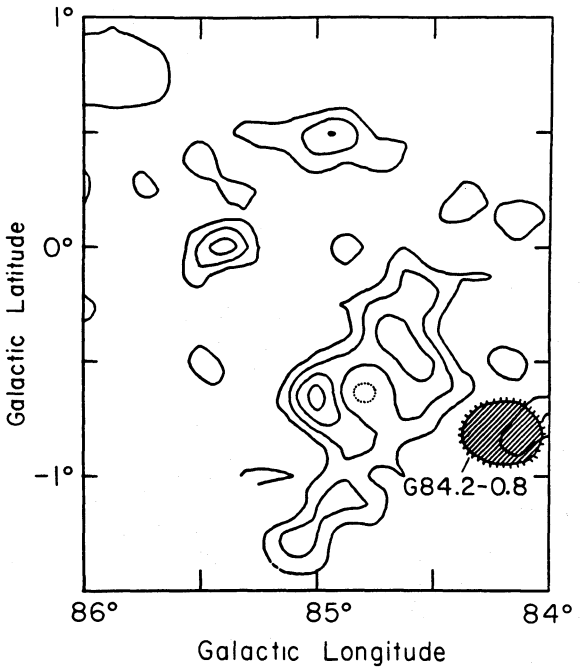

FIG. 2.—SNR G84.2−0.8; map integrated over velocity from −55 to −30 km s^{-1} with a contour interval of 4.5 K km s^{-1}.

higher longitude (Fig. 2). Adopting the mean kinematic distance of 7.2 kpc to the cloud complex, the total mass is $8.5 \times 10^5\ M_\odot$. The cloud was missed by previous CO surveys of Bally and Scoville (1980) and Dame and Thaddeus (1985) because of their low sensitivity and low resolution respectively. The near spatial coincidence between this cloud complex and G84.2−0.8 makes an association between the two objects likely.

G89.0+4.7 (HB 21).—A molecular cloud complex with a peak velocity near 0 km s^{-1} partially surrounding the shell-like SNR HB 21 at a Σ-D distance of 1.2 kpc (Table 1) was found by the 1° resolution CO survey of Dame and Thaddeus (1985). Figure 3, combining the 0°.5 resolution survey of Gottlieb, Brock, and Thaddeus (1985) at $l > 98°$ with the survey of Dame and Thaddeus at $l \leq 98°$, shows the overall structure of the nearby molecular gas.

The cloud complex is associated with Cyg OB7 ($l = 84°$–$96°$, $b = -4°.9$ to 9°) and Cep OB2 ($l = 97°$–$108°$, $b = -0°.9$ to 12°.3) at a distance of ~0.8 kpc (Humphreys 1978), which implies a total mass of $6.9 \times 10^5\ M_\odot$ to the complex. As noted in the survey of Gottlieb, Brock, and Thaddeus (1985), a velocity shift of 8 km s^{-1} and relatively large velocity widths (up to an FWHM of 10 km s^{-1}) appear in the immediate vicinity of the bright H II region S131 excited by the embedded young open cluster IC 1396 comprising the core of Cep OB2. These phenomena, possibly resulting from an interaction of the H II region and the ambient cloud complex, strengthen a possible relation between the cloud complex and both Cep OB2 and Cyg OB7. Owing to their proximity, the progenitor of HB 21 may have originated from Cyg OB7.

G93.3+6.9 (DA 530).—Once thought to have a filled center, DA 530 was recently shown to be shell-like (Lalitha *et al.* 1984). Its Σ-D distance, 5.7 kpc (Table 1), yields a displacement of 690 pc above the Galactic plane, so large that a Type I origin is suggested (Roger and Costain 1976).

Weak CO emission with V_{LSR} from −5 to 0 km s^{-1} (Fig. 4), most likely from the cloud complex associated with Cyg OB7 and Cep OB2 at ~0.8 kpc (see discussion of HB 21, above), appears in the vicinity of DA 530. The SNR is apparently located behind the cloud complex, because neither the POSS plates nor the emission-line survey of Parker, Gull, and Kirshner (1979) shows the optical remnant.

G93.7−0.3 (CTB 104A).—The radio source CTB 104A is a peculiar remnant with a thick shell and a central condensation (Landecker, Higgs, and Roger 1984), whose Σ-D distance is 1.8 kpc (Table 1).

We observed a 6° × 5° rectangle centered on the plane at $l = 94°.5$ in order to cover CTB 104A as well as nearby SNR 3C 434.1. Several cloud complexes with velocities from −60 to 15 km s^{-1} appear in the line of sight. The local cloud complex ($V_{LSR} \approx 0$ km s^{-1}), part of the large complex associated with Cep OB2 and Cyg OB7 at 0.8 kpc, may be located in front of CTB 104A, because the POSS plate and the emission-line survey of Parker, Gull, and Kirshner (1979) do not show the optical remnant. Another cloud complex (Fig. 5*a*) with a peak velocity of ~ −14 km s^{-1} (and a total mass of $2.3 \times 10^5\ M_\odot$ if a kinematic distance of 2.8 kpc is assumed) displays an unusually clumpy structure, possibly the result of disruption of a once larger cloud. The most distant cloud complex detected ($V_{LSR} = -55$ to −35 km s^{-1}; Fig. 5*b*) is located at 3.6 kpc (the

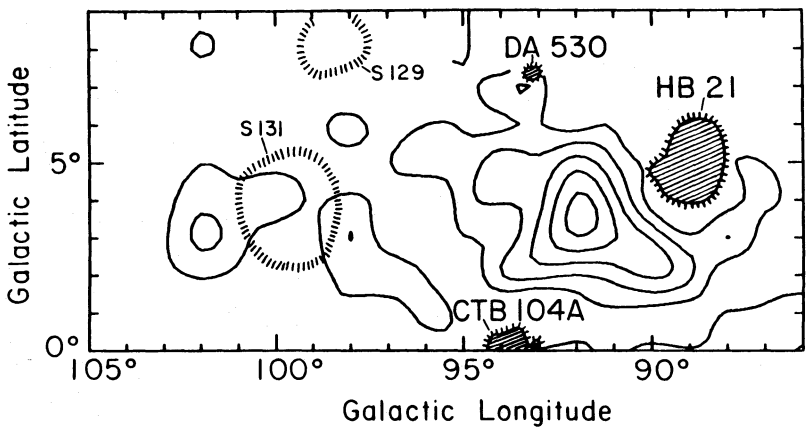

FIG. 3.—HB 21 and DA 530; map smoothed to angular resolution of 1° and integrated over velocity from −15 to 10 km s^{-1} with a contour interval of 4.5 K km s^{-1}.

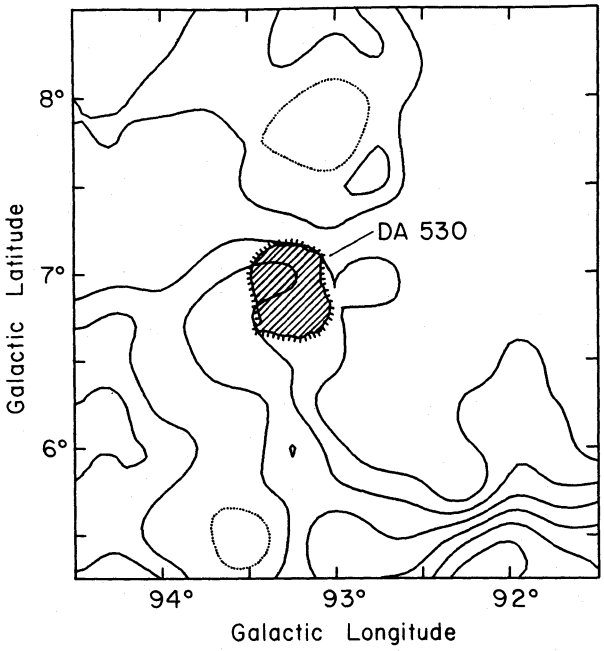

FIG. 4.—DA 530; map integrated over velocity from −10 to 10 km s^{-1} with a contour interval of 3 K km s^{-1}.

spectrophotometric distance of the associated H II region S 124; Chini and Wink 1984), yielding a mass of $5.3 \times 10^5 M_\odot$. Owing to the large uncertainty in the distance to the SNR, either of these two more distant cloud complexes may be a candidate for the birthplace of the progenitor of CTB 104A.

G94.0+1.0 (3C 434.1).—Recent high-resolution radio observations of Landecker, Higgs, and Roger (1984) show this SNR to be shell-like, not Crablike as previously thought. The Σ-D distance of the remnant is 4.7 kpc (Table 1). The existence of two large molecular cloud complexes in the line of sight (see CTB 104A, above), one at 2.8 kpc, the other at 3.6 kpc, makes assignment of the birthplace of the progenitor of 3C 434.1 ambiguous.

G109.2−1.0 (CTB 109).—The Σ-D distance to CTB 109 is 4.1 kpc (Table 1). The GISS–Columbia CO surveys of the second quadrant (Cohen *et al.* 1980; Gottlieb, Brock, and Thaddeus 1985), supplemented by a few new observations, reveal an elongated cloud with peak velocities from −57 to −46 km s^{-1} at the edge of CTB 109 (Fig. 6).

Gregory *et al.* (1983) have suggested that the shock wave of the SNR is expanding into the cloud, so we checked the velocity structure of the cloud for evidence of interaction. A velocity gradient of ~5 km s^{-1} deg^{-1} appears along the major axis of the cloud, but there is little reason to think that it results from an interaction, since the line width is small and the velocity gradient extends over the whole cloud. Slow rotation with a

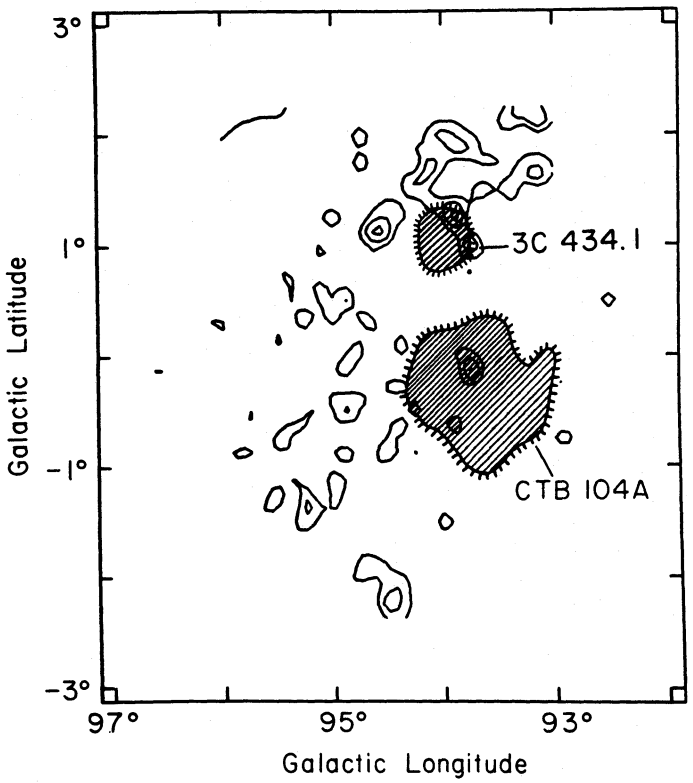

FIG. 5a

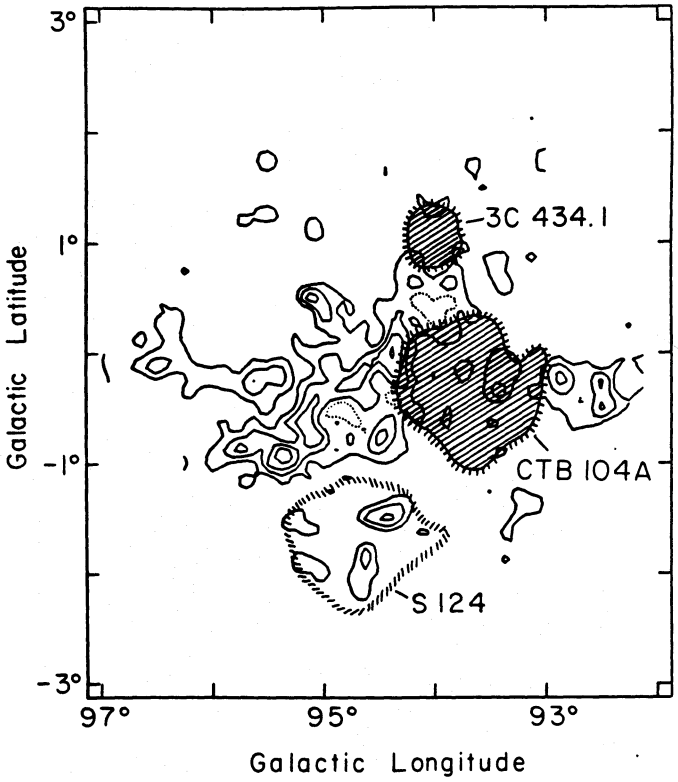

FIG. 5b

FIG. 5.—CTB 104A and 3C 434.1. (*a*) Map integrated over velocity from −25 to −10 km s^{-1} with contour interval of 2.5 K km s^{-1}. (*b*) Integrated over velocity from −55 to −35 km s^{-1} with a contour interval of 2.5 K km s^{-1}.

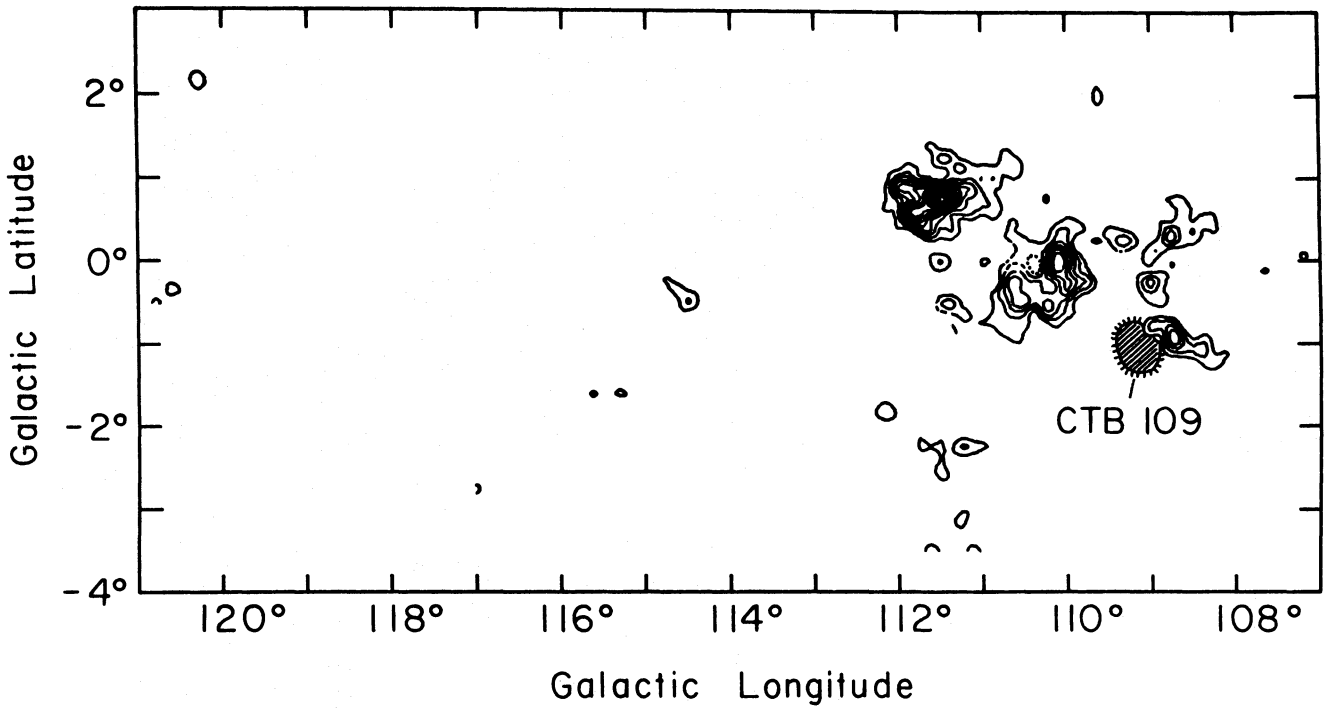

FIG. 6.—CTB 109 and Cep OB1 association; brightest CO-emitting regions associated with Cep OB1 ($l = 98°$–$108°$, $b = -3°$ to $-0.°7$; Humphreys 1978). Integrated over velocity from -60 to -45 km s^{-1}, in steps of 7.5 K km s^{-1}. More than 2000 points within this map have been observed by various observers with the GISS–Columbia telescope.

period of $\sim 10^8$ yr around its minor axis is adequate to account for this velocity gradient. Although we found little evidence of interaction, the spatial coincidence suggests that this cloud is likely to be the birthplace of the stellar progenitor of CTB 109.

A chain of five small H II regions (S147, S148, S149, S152, and S153) in the direction of this cloud at about the same radial velocity (Recillas-Cruz and Pismis 1979; Pismis and Hasse 1980) may be related. Estimates of spectrophotometric distances to the H II regions vary significantly, from 3.6 to 9.6 kpc (see, e.g., Recillas-Cruz and Pismis 1979; Pismis and Hasse 1980; Wramdemark 1981), but because the cloud is probably part of the Cep OB1 cloud complex at 3.5 kpc (Humphreys 1978; Fig. 6) owing to their proximity, the lower limit is a more likely estimate. At 3.5 kpc, the total mass of the cloud complex is calculated to be $1.7 \times 10^6\ M_\odot$. The complex may be the outer part of the Perseus arm bifurcation in this direction (Verschuur 1973), the Cas OB2 cloud complex being located at a closer distance (~ 2.6 kpc; see discussion of Cas A, next).

G111.7−2.1 (*Cas A*).—The distance to this strong shell-like SNR is 2.8–3.1 kpc (van den Bergh 1971; Sakhibov 1980), derived from a comparison of the radial velocities and the proper motions of its optical filaments. Cas A lies at the edge of the Cas OB2 association ($l = 110.°1$–$114°$, $b = -1.°3$ to $1.°8$), which is at a comparable distance of 2.6 kpc (Humphreys 1978).

With a total mass of $6.8 \times 10^5\ M_\odot$, the Cas OB2 cloud complex (Fig. 7) is one of the largest in the Perseus Arm. The velocity structure of the complex in the immediate vicinity of Cas A is complicated: multiple components appear at from -47 to -38 km s^{-1}, in contrast to the main feature at $V_{LSR} \approx -38$ km s^{-1}. This velocity structure possibly results from the activity of a faint H II region (Minkowski 1968) located near the center of the SNR and may be associated with the complex. The spatial proximity suggests that the Cas OB2 complex is the plausible birthplace of Cas A.

G114.3+0.3.—Three SNRs, G114.3+0.3, G116.5+1.1, and CTB 1, cluster within 2° of one another (Fig. 8), but the relationship between them is unclear. The small H II region S165 is located within the outline of G114.3+0.3, whose Σ-D distance is 3.0 kpc (Table 1). Failure to detect depolarization or Faraday rotation effects from the 21 cm continuum survey of the SNR led Reich and Braunsfurth (1981) to suggest that the remnant is in front of the H II region, but a precise distance to the remnant cannot be established because of the large uncertainty in the distance to S165.

The velocities of the small molecular clouds in Fig. 8 suggest that some are related to the Cep OB1 cloud complex (3.5 kpc) and some related to the Cas OB2 cloud complex (2.6 kpc); at these distances all have masses much less than $10^5\ M_\odot$.

G116.5+1.1.—The projected location of this SNR, at a Σ-D distance of 3.1 kpc (Table 1), is at the adjacent boundaries of Cas OB4 ($l = 119°$–$121.°6$, $b = -2.°1$ to $2°$) and Cas OB5 ($l = 114.°9$–$118°$, $b = -2.°1$ to $2°$), at 2.9 and 2.5 kpc (Humphreys 1978) respectively. Whether the SNR is related to either Cas OB4 or Cas OB5 remains open. Other than a local feature, no significant CO emission was detected in the immediate vicinity of the SNR (Fig. 8).

G116.9+0.2 (*CTB 1*).—This SNR, at a Σ-D distance of 4.5 kpc (Table 1), is embedded in an extensive, faint H II region (Willis and Dickel 1971). Although no direct evidence exists, Dickel and Willis (1980) suggest CTB 1 is the remnant of an SN that resulted from the H II region. The mean Hα velocity (-35 ± 10 km s^{-1}; Lozinskaya 1981) of the filaments of CTB 1 implies a kinematic distance of 2.6 ± 0.7 kpc, assuming a flat

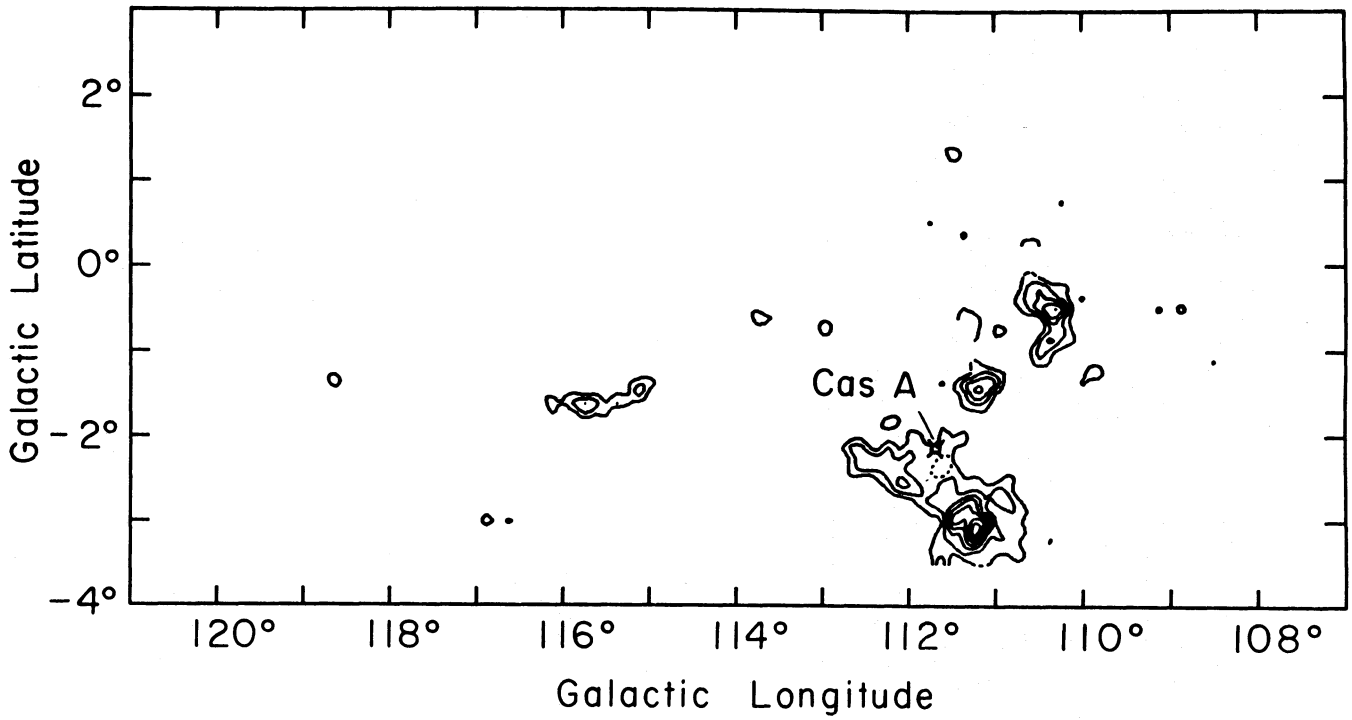

FIG. 7.—Cas A and Cas OB2 association; brightest CO-emitting regions associated with Cas OB2 ($l = 110°.1$–$114°$, $b = -1°.3$ to $1°.8$; Humphreys 1978). Integrated over velocity from -45 to -30 km s^{-1}, in steps of 7.5 K km s^{-1}. Cas A is indicated by the spoked square symbol.

rotation curve. This estimate does not include the uncertainty that results from the possible noncircular motions in this direction (Rickard 1968).

No significant CO emission is detected at the boundary of the SNR (Fig. 8).

G119.5+9.8 (CTA 1).—The Σ-D distance of CTA 1 is 1.9 kpc (Table 1); a lower limit of 0.9 ± 0.1 kpc (Acker 1978) can be set from a possible depolarization toward NGC 40 (Sieber, Haslam, and Salter 1979), a planetary nebula lying on the southeastern ridge of the radio continuum of the remnant.

A cloud complex at a velocity of ~ -3 km s^{-1} was found partially surrounding the remnant (Fig. 9). Its main body coincides with a faint dust lane (Fesen *et al.* 1981) extending from northwest to southeast. A weak CO feature appears in the northwestern quadrant of the remnant, where no optical filament is detected. Although this feature might hamper the

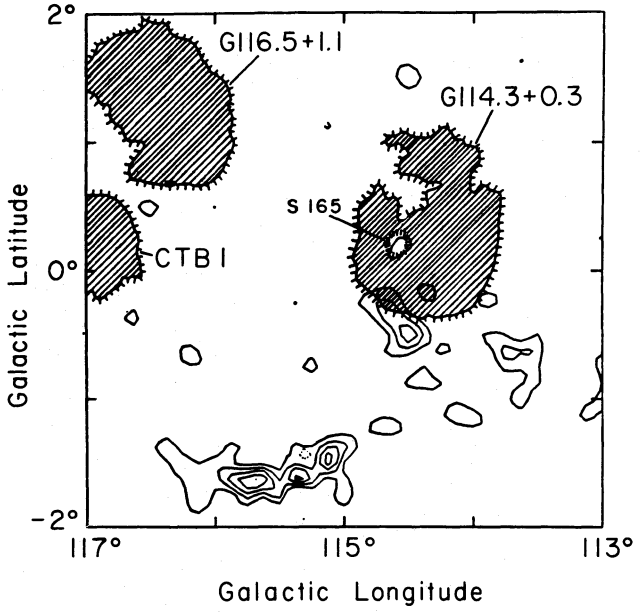

FIG. 8.—G114.3+0.3, G116.5+1.1, and CTB 1; contours integrated over velocity from -55 to -35 km s^{-1} and in steps of 5 K km s^{-1}.

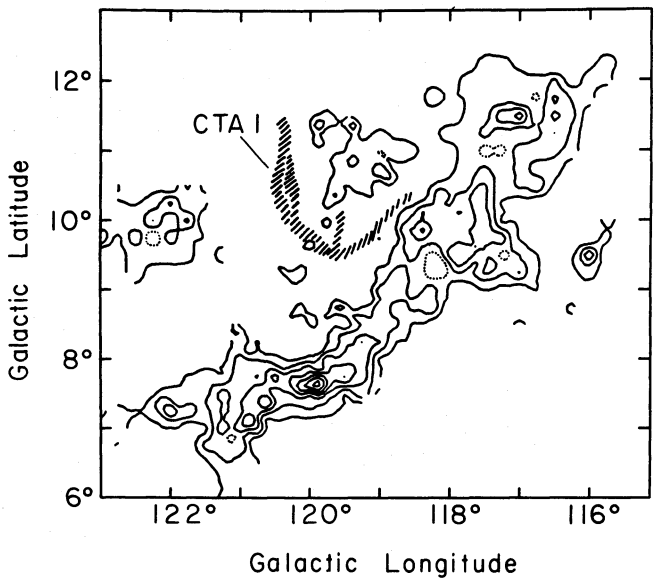

FIG. 9.—CTA 1; map integrated over velocity from -7 to 2 km s^{-1} with a contour interval of 2.5 K km s^{-1}.

detection of optical emission, the discontinuity of the radio shell in this quadrant (see, e.g., Sieber, Salter, and Mayer 1981) argues against the existence of optical filaments here. Owing to the low velocity, the kinematic distance to the cloud complex is unreliable. Whether the cloud complex around CTA 1 is related to the stellar association Cep OB4 ($l = 117.^{\circ}4$–$118.^{\circ}6$, $b = 3.^{\circ}9$–$6.^{\circ}5$; Humphreys 1978) located $\sim 3^{\circ}$ away remains unclear. If the complex near CTA 1 and the cloud complex associated with Cep OB4 (Gottlieb, Brock, and Thaddeus 1985) comprise a single star-forming complex, the total mass is estimated to be $3.0 \times 10^5\ M_{\odot}$, assuming a distance of 0.8 kpc (MacConnell 1968).

G120.1+1.4 (Tycho's SNR).—The most negative H I absorption feature toward this often-studied remnant is at -52 or -60 km s^{-1} (Schwarz, Arnal, and Goss 1980; Albinson and Gull 1982). A flat rotation curve gives a lower limit of 4.9–5.8 kpc for its distance; but large, noncircular motions in this direction (e.g., Rickard 1968) may allow the distance to be as small as 2 kpc (Black and Raymond 1984)—consistent with the estimate of 2.3 ± 0.5 kpc calculated from the shock velocity and proper motion of filaments of the SNR (Chevalier, Kirshner, and Raymond 1980).

There is a molecular cloud at $V_{LSR} = -62$ km s^{-1} toward Tycho's remnant (Fig. 10), a small part of which was previously detected by Cornett (1977), working at an angular resolution of 1′, who suggested an interaction between the SNR and the CO cloud based on velocity shift and line-width broadening. This suggestion is questionable because the line width he observed (~ 6 km s^{-1}) is much narrower than the expected width of shocked CO (a few tens of km s^{-1}).

The small H II region S175, excited by an O9.5 V star at 1.7 kpc (Georgelin 1975), is located midway between two CO features at -50 and -62 km s^{-1} respectively (Fig. 10). There is no evidence from broad-winged emission of bipolar outflow in our data.

G126.2+1.6.—This SNR is located adjacent to the SNR G127.1+0.5 (Fig. 11) on the plane of the sky; its Σ-D distance is 3.6 kpc (Table 1). A search for evidence of star formation led to a faint H II region DU 65 (Dubout-Crillon 1976; Fig. 11) of unknown distance located roughly 1° away from its boundary.

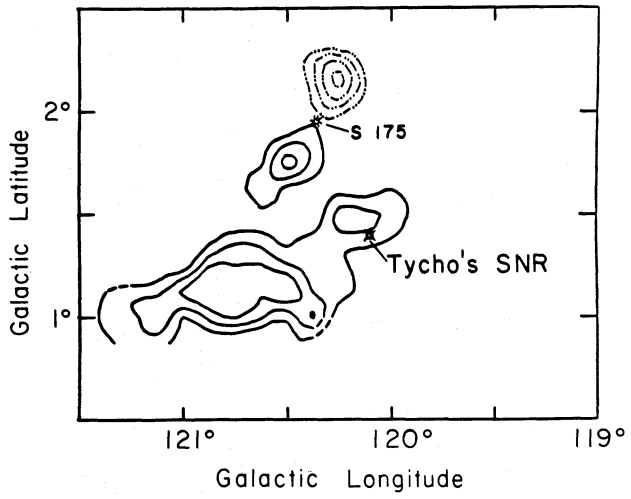

FIG. 10.—Tycho's SNR, solid contours integrated over velocity from -70 to -55 km s^{-1}. The emission integrated from -55 to -45 km s^{-1} is marked by dash-dot lines. For both, the contour intervals are 3 K km s^{-1}. The H II region S175 lies between two CO features in the projected plane of the sky.

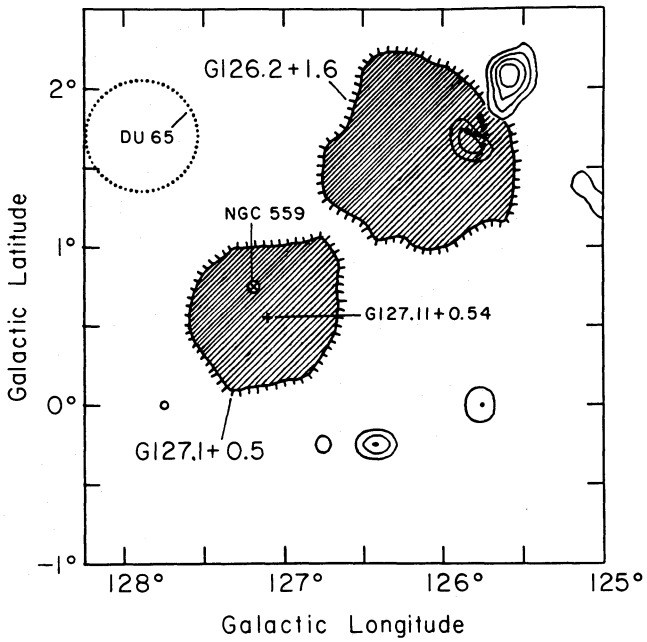

FIG. 11.—G126.2+1.6 and G127.1+0.5; map integrated over velocity from -70 to -50 km s^{-1} with a contour interval of 2 K km s^{-1} and a temperature cutoff at 1 K.

Two small CO features lie near the remnant, one ($V_{LSR} = -54$ km s^{-1}) just outside its northwest boundary, the other ($V_{LSR} = -65$ km s^{-1}) toward the optical filaments discovered by Blair *et al.* 1980). Although the proximity in projected position favors an association between the SNR and either feature, a chance coincidence cannot be ruled out.

G127.1+0.5.—This SNR, at a Σ-D distance of 3.5 kpc (Table 1), is located in region free of any large CO cloud (Fig. 11). The open cluster NGC 559 (at 1.3 kpc; Lindoff 1969) within the boundaries of the remnant is probably an unrelated foreground object, because its distance is significantly smaller than the Σ-D distance of the SNR and because no optical remnant is observed in the line of sight (Blair *et al.* 1980), where little extinction is expected (our survey detected only weak local CO emission).

The strong compact source G127.11+0.54 at the center of the SNR is especially interesting. A large redshift in its optical spectrum suggests it may be an obscured galaxy (e.g., Spinrad, Stauffer, and Harlan 1979), but the possibility that it is a Galactic SS 433–like star has been considered (Geldzahler and Shaffer 1982). The coincidence in position may result merely from chance, because the most negative H I absorption feature at -92 km s^{-1} toward the compact source (Pauls *et al.* 1982) suggests it is at least 10.7 kpc away, and at this distance the SNR would be extremely large, at least twice as large as the next largest SNR in the Galaxy (see Milne 1979).

G130.7+3.1 (3C 58).—This SNR is one of the few Crablike remnants in the Galaxy. The corresponding radial velocity, derived from H I absorption, has recently been revised from -95 km s^{-1} or less (see, e.g., Hughes, Thompson, and Colvin 1971) to -37 km s^{-1} (Green and Gull 1982), as the result of observations with the Cambridge Half-Mile Telescope. This less negative velocity, which, similar to that of the Cas OB6 cloud complex (at a photometric distance of 2.2 kpc; Humphreys 1978) at $\sim 3^{\circ}$ away (Fig. 12), implies a distance of roughly 2.2 kpc to the SNR.

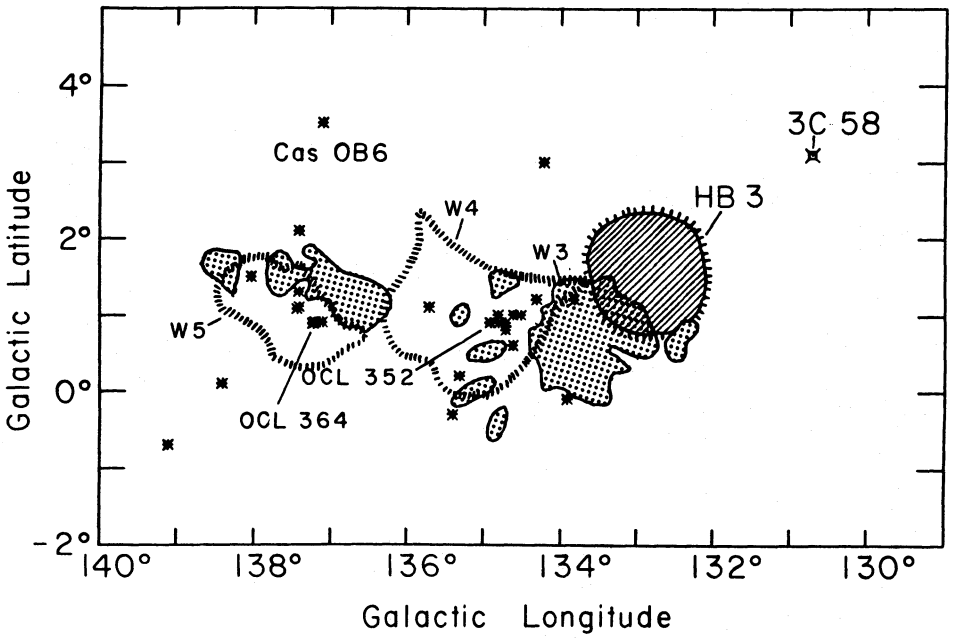

FIG. 12.—3C 58 and HB 3; the molecular cloud complex detected in Lada *et al.* (1978) is denoted by the dotted regions and the most luminous members of Cas OB6 by stars.

Our CO observations near 3C 58 detected only a weak local emission at $V_{LSR} = -7$ km s^{-1}.

G132.7+1.3 (HB 3).—This SNR lies at the far western edge of the Cas OB6 cloud complex, an active star-forming region in the Perseus arm, which contains the bright H II regions W3, W4, and W5 and the open clusters OCL 352 and OCL 364 (Fig. 12). The agreement between the CO velocities of the cloud complex and the mean Hα velocity of the optical filaments of HB 3 (Lozinskaya and Sitnik 1980) clearly permits an association between the two objects.

We observed an area near the SNR and the H II regions W3 and W4 with a better sensitivity and better spectral resolution than the previous survey done by H.-I. Cong (Lada *et al.* 1978) using the same telescope. Generally, both these CO surveys agree, except for our detection of faint molecular gas at $l = 132.^{\circ}3$, $b = 0.^{\circ}7$ (Fig. 13), missed in Cong's survey. Adopting a distance of 2.2 kpc, the distance to Cas OB6 (Humphreys 1978), the total mass of the cloud complex near W3 and W4 is calculated to be $2.9 \times 10^5\ M_{\odot}$. A velocity gradient on the order of 8 km s^{-1} is evident over the main cloud which may be a result of rotation.

G160.4+2.8 (HB 9).—Our CO observations detected a cloud complex with $V_{LSR} = -21$ km s^{-1} at the northern portion of HB 9 (Fig. 14). The complex probably lies in front of the remnant, because the optical filaments appear only where no CO emission was detected, while radio observations (e.g., Reich 1983) reveal a complete, rather than a partial, shell. A search for evidence of star formation toward the cloud complex found two associated H II regions, S217 and S219 (Fig. 14), both with Hα velocities similar to the CO velocity (Table 2). If the mean Hα velocity of the filaments of HB 9 is roughly at -18 km s^{-1} (with an uncertainty of ± 10 km s^{-1}; Lozinskaya 1981), the progenitor of the SNR may have originated from the cloud complex. Adopting the mean spectrophotometric distance of 5.6 kpc to the H II regions (Table 2), the cloud mass is calculated to be $5.4 \times 10^5\ M_{\odot}$.

G166.1+4.4 (VRO 42.05.01) and G166.3+2.5 (OA 184).—It

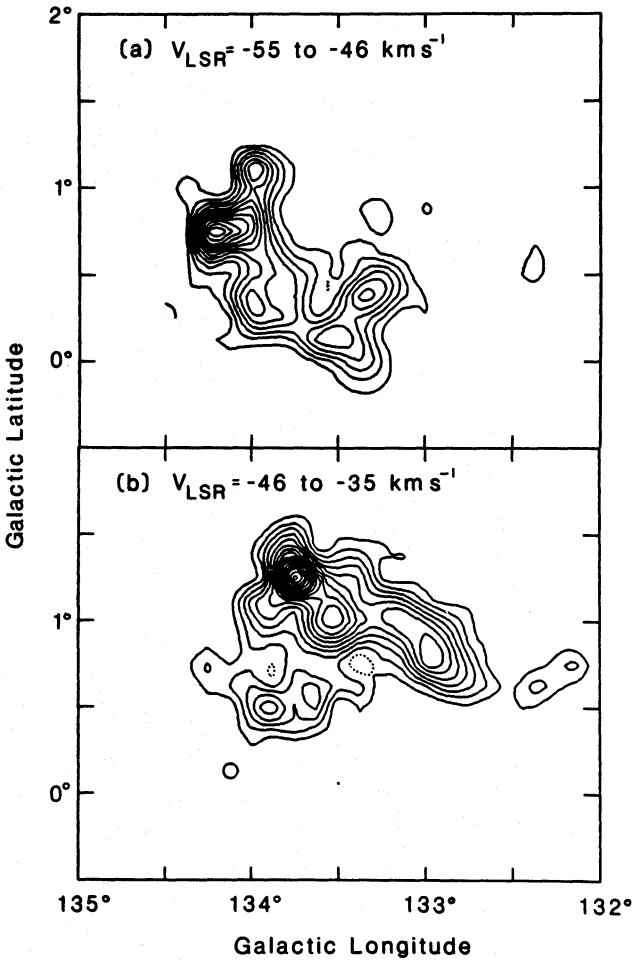

FIG. 13.—HB 3, maps integrated over velocity from (*a*) -55 to -46 km s^{-1} and (*b*) -46 to -35 km s^{-1}. The contour intervals are 3 K km s^{-1} for both.

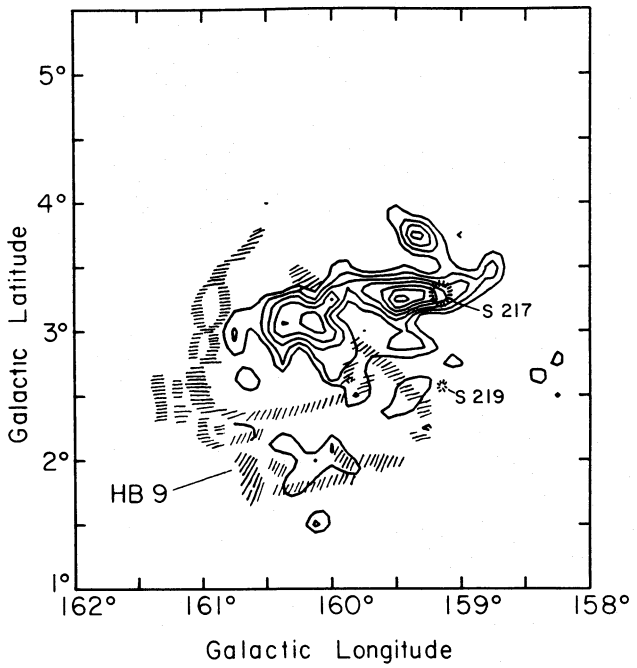

FIG. 14.—HB 9, map integrated over velocity from −30 to −12 km s^{-1} with a contour interval of 2 K km s^{-1}.

has been suggested that the peculiar shape of VRO 42.05.01, an almost complete circular shell with a wing, is the result either of a single SNR evolving in two regions of sharply different densities or of two successive SNs (Landecker *et al.* 1982*a*). Another SNR, OA 184 (Fig. 15), lies ∼2° south of VRO 42.05.01; the Σ-*D* distances of VRO 42.05.01 and OA 184, at 4.1 and 3.1 kpc (Table 1) respectively, are comparable.

A cloud complex with a velocity of −22 km s^{-1} lies between VRO 42.05.01 and OA 184 (Fig. 15), probably located in the same vicinity because the radial velocities of the two SNRs and the complex are close (Table 3). A search for neighboring optical young objects reveals a small H II region S225 (Fig. 15) with a spectrophotometric distance of 3.7–4.0 kpc (Table 3). Whether S225 is associated with the cloud complex remains unclear, because its radial velocity is unknown and the H II region is located ∼0°.7 away from the nearest cloud boundary. The next nearest H II region, S228 (G169.2−0.9), has a CO velocity of −16 km s^{-1} at a spectrophotometric distance of 4.7 kpc (Table 3). Since the longitude and velocity of S228 are similar to those of the complex, we adopt a distance of 5 kpc to

TABLE 2

PARAMETERS OF SNR HB 9 AND H II REGIONS S217 AND S219

Object	*l*	*b*	*V* (CO) (km s^{-1})	*V* (Hα) (km s^{-1})	Spectrophotometric Distances (kpc)
S217	159°.2	3°.3	−20[a]	−21[b]	5.6,[c] 4.3,[b] 5.2,[d] 7.1[e]
S219	159.4	2.6	−25[a]	−25[b]	6.3,[c] 5.3,[b] 4.2[d]
HB 9	160.4	2.8	...	−18±10[f]	...

[a] This work.
[b] Georgelin 1975.
[c] Georgelin *et al.* 1973.
[d] Moffat *et al.* 1979.
[e] Chini and Wink 1984.
[f] Lozinskaya 1981.

TABLE 3

YOUNG OBJECTS NEAR $l \approx 166°$

Object	*l*	*b*	*V* (Hα) (km s^{-1})	*V* (CO) (km s^{-1})
VRO 42.05.01	166°.1	+4°.4	−21±4[a]	...
OA 184	166.3	+2.5	−22[b]	...
S225	168.1	+3.1	...	...
S228	169.2	−0.9	...	−16[c]
CO cloud	...	...	...	−22[d]

[a] Arsenault and Roy 1984.
[b] Lozinskaya 1981.
[c] Blitz *et al.* 1982.
[d] This work.

the complex, yielding a total mass of 1.3 × 10^5 $M_\odot$. The hypothesis that two successive SNs in the same field produced SNR VRO 42.05.01 may be more plausible, because our CO data did not show sharply different densities on the face of the remnant.

G180.3−1.7 (*Simeis 147; Shajn 147*).—This large angular sized (∼3° in diameter) SNR located toward the Galactic anticenter displays remarkable filamentary optical features (see, e.g., van den Bergh 1978). Kirshner and Arnold (1979) and Kundu *et al.* (1980) derived a distance of 0.6–0.8 kpc from the expansion velocity of the filaments, comparable to the Σ-*D* distance of 1.4 kpc (Table 1). Although our 0°.5 resolution survey detected several CO features near Simeis 147, the location of these features close to the Galactic anticenter precludes useful estimates of distance from any rotation curve (forbidden velocities of up to 18 km s^{-1} deviating from the circular motion appear in our survey). A weak cloud (toward HD 36665) with a peak velocity of 4 km s^{-1}, close to the mean Hα velocity of 9±4 km s^{-1} of the optical filaments (Lozinskaya 1976), lies in the direction of the SNR (Fig. 16). Detection of low-velocity interstellar CO absorption features in the UV spectrum toward HD 36665 (at a distance of 0.9 kpc; Phillips, Gondhalekar, and Blades 1981) implies that the cloud is located in front of the star. Whether the cloud is associated with the SNR remains unknown, but it probably does lie in

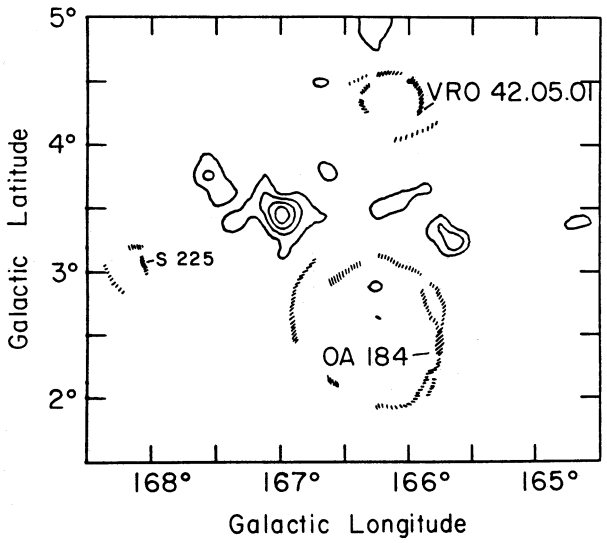

FIG. 15.—VRO 42.05.01 and OA 184; map integrated over velocity from −30 to −15 km s^{-1} with a contour interval of 2.5 K km s^{-1}.

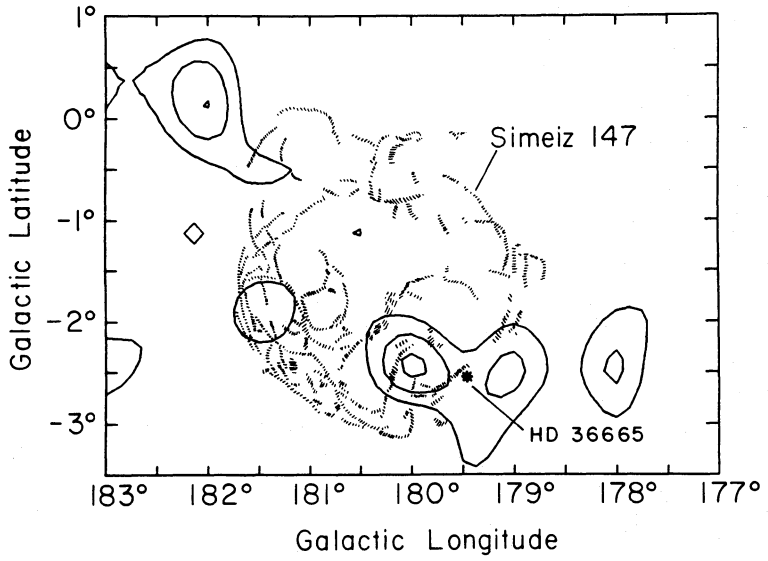

FIG. 16.—Simeis 147, map integrated over velocity from 0 to 10 km s^{-1} with a contour interval of 2.5 K km s^{-1}. The B2e star HD 36665 is indicated.

front of the SNR, because a dust lane can barely be seen against the optical filaments in the line of sight (see Minkowski's photo in van den Bergh, Marscher, and Terzian 1973).

G184.6−5.8 (Crab Nebula; SN 1054).—Using various methods, the distance for this remnant has been estimated to be from 1.4 to 2.7 kpc (Trimble 1973). Attempts to classify the type of SN 1054 from historical records, based on the inferred light curves or maximum absolute magnitude, run the gamut from Type I (Mayall and Oort 1942), to neither type (Minkowski 1971), to Type II (Chevalier 1977), and again to Type I *slow* (Brandt and Williamson 1979). It may not be possible to unambiguously assign the Crab Nebula a type based on inaccurate pretelescopic data, because a light curve cannot unambiguously determine the type of an SN (Doggett and Branch 1985) and because the maximum absolute magnitudes of Types I and II SNs overlap at ~ -18 mag (Tammann 1982), the inferred magnitude of the Crab Nebula.

Our 8′ resolution survey detected only one cloud complex with $V_{LSR} = 7$ km s^{-1} at 2° away from the remnant (see Fig. 17), and this cloud complex, revealing a large extension of $\sim 6°$ in the 0°.5 resolution survey, a small velocity width (FWHM ≈ 2 km s^{-1}), and a sharp temperature drop at the edge, is likely to be only a local feature. The appearance of H I absorption features up to ~ 15 km s^{-1} in the direction of the Crab Nebula (Greisen 1973) also supports a foreground origin for the cloud complex. The Gem OB1 cloud complex, located 6° away at a comparable distance of 1.5 kpc (see discussion of IC 443), is the most plausible birthplace for the progenitor of the Crab Nebula.

G189.0+3.0 (IC 443).—Estimated distances to this SNR range from 0.5 to 2.5 kpc (see Fesen and Kirshner 1980, and references therein). A CO cloud with a peak velocity of ~ -4 km s^{-1} found toward the remnant may be in front, because the CO emission shows an anticorrelation in projected position with the optical filaments (Scoville *et al.* 1977; Cornett, Chin, and Knapp 1977). Detection of apparently shocked gas (see Huang, Dickman, and Snell 1986, and references therein) suggests an interaction between the cloud and the SNR.

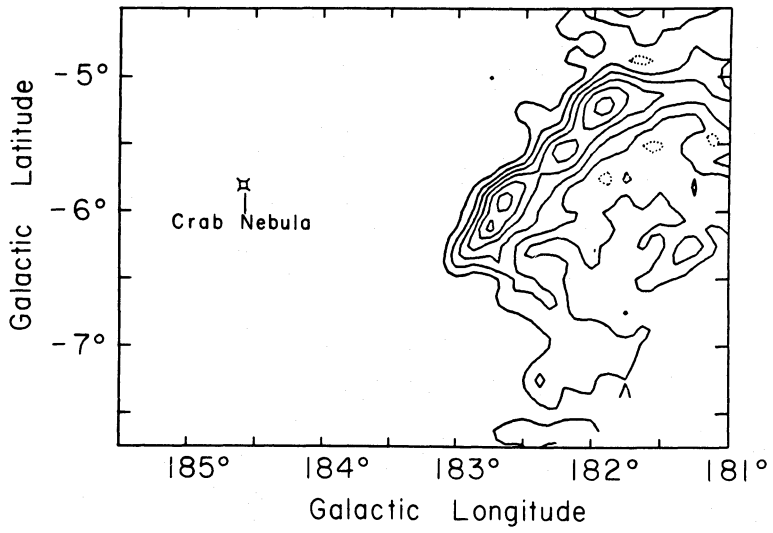

FIG. 17.—Crab Nebula, map of the peak CO temperatures within the velocity range of 0–10 km s^{-1}. The contour interval is 1 K.

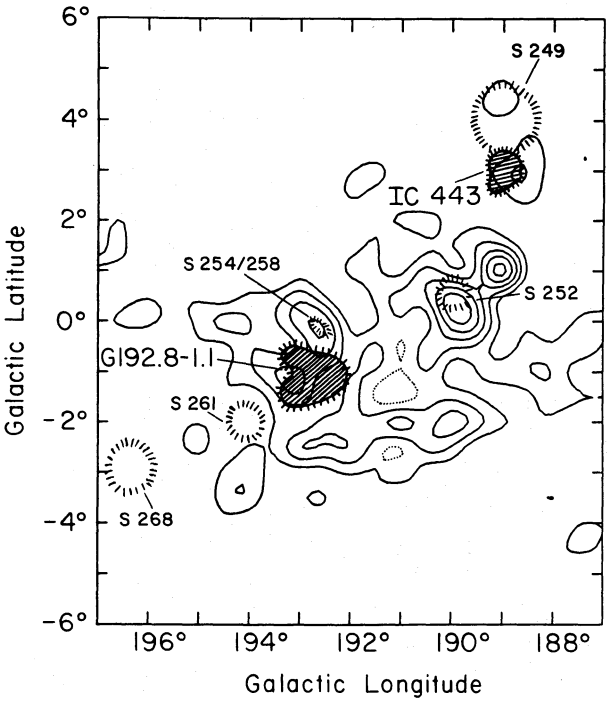

FIG. 18.—IC 443 and G192.8 − 1.1; CO emission associated with Gem OB1 (l = 187°.4–190°.8, b = −2°.1 to 4°.2; Humphreys 1978). Map integrated over velocity from −10 to 12 km s^{-1} with a contour interval of 4 K km s^{-1}.

In our 0°.5 resolution survey, this cloud appears to be part of the large cloud complex associated with Gem OB1 (l = 187°.4–190°.8, b = −2°.1 to 4°.2; Fig. 18). Many H II regions (see Fig. 18) with spectrophotometric distances of from 1.5 to 2.5 kpc lie in the direction of the cloud complex, and, within uncertainties, these distances agree with the distance (1.5 kpc; Humphreys 1978) of Gem OB1. At 1.5 kpc, the total mass of the Gem OB1 cloud complex is calculated to be 1.3 × 10^6 $M_\odot$.

G192.8 − 1.1.—Although this radio source was formerly considered part of the questionable SNR Ori-Gem Loop, Caswell (1985) suggests it is an independent SNR. Its Σ-D distance of 2.6 kpc (Table 1) agrees, within uncertainties, with the spectrophotometric distance (1.5 kpc) of the Gem OB1 cloud complex in this direction (Fig. 18).

G205.6 − 0.1 (*Monoceros Loop*).—This large SNR (a diameter of ∼4°), with Mon OB2 and the related Rosette nebula to the southwest and with Mon OB1 and the related Cone nebula to the north (Fig. 19*a*), shows a faint ringlike optical feature. Its Σ-D distance of 0.8 kpc (Table 1) agrees, within uncertainties, with the distance of either Mon OB2 (1.6 kpc) or Mon OB1 (0.8 kpc) (Turner 1976). Although the Hα line widths are smaller near the center of the Rosette nebula than near the SNR and this difference has been interpreted as an interaction between them (Fountain, Gary, and O'Dell 1979; Vidal-Madjar *et al.* 1982), the evidence is not solid enough to rule out unambiguously an association of the remnant with Mon OB1.

With the GISS–Columbia telescope, Blitz (1978) detected extensive emission related to Mon OB1 and Mon OB2, at peak velocities of ∼6 and 15 km s^{-1} respectively. Our 0°.5 resolution survey, which provides the first map of the large-scale distribution of molecular gas in this general direction (Fig. 19*b*), shows only a few weak features other than the prominent Mon OB1 and Mon OB2 cloud complexes. No strong CO emission appears toward the Monoceros Loop.

G206.9 + 2.3 (*PKS 0646 + 06*).—Located immediately next to the main shell of the Monoceros Loop (Fig. 20), this faint radio source is a physically distinct SNR (van den Bergh 1978) with a Σ-D distance of 4.3 kpc (Table 1). CO observations in the vicinity of PKS 0646 + 06 show clumpy weak features, most of them apparently part of the Mon OB2 cloud complex. The clumpy structure may be the result of cloud dissipation of member stars in the oldest subgroup of Mon OB2 in this area (Turner 1976). The SNR PKS 0646 + 06 may be a background object unrelated to the Mon OB2 cloud complex.

The available CO surveys, mainly this one, reveal large molecular cloud complexes in the direction of many SNRs. More specifically, the SNRs are located at the boundaries of the cloud complexes, not deeply embedded in the clouds. This is consistent with the observational bias that most SNs exploded in the cloud complexes may have been missed by previous SNR surveys, because their angular resolutions are not good enough to detect such remnants, which are of small sizes even at their late stages of evolution (Kafatos *et al.* 1980).

The large cloud complexes located in the vicinity of the SNRs, except those distant ones obscured by heavy foreground extinction, generally shown evidence of massive star formation from the appearance of accompanying OB associations or H II regions. These large complexes may be responsible for the birth of most massive stars (Myers *et al.* 1986) and presumably are the birth places of the progenitors of SNs (especially Type II).

However, even though many SNRs present spatial coincidences with large cloud complexes, no direct evidence (e.g., detection of shocked CO) of an association between any particular SNR and a large cloud complex is shown in our data. The beam dilution of the GISS–Columbia telescope may have washed out any signs of shocked CO emission, which is generally weak and has a large line width on the order of a few tens of km s^{-1} (see Huang, Dickman, and Snell 1986, and references therein). Clear evidence of an association between an SNR and a large molecular cloud complex may be intrinsically difficult to obtain for some SNRs, because their progenitors migrated away from the parent clouds before explosion. To answer whether SNs (presumably Type II) preferentially occur near large molecular cloud complexes, or whether the apparent spatial coincidences we observed between SNRs and large cloud complexes are merely the result of chance, we made the statistical study, discussed next.

IV. STATISTICAL STUDY OF THE ASSOCIATION OF SUPERNOVA REMNANTS WITH MOLECULAR CLOUDS

The statistical study requires knowledge of the distribution of molecular clouds beyond the solar circle. Table 4 summarizes the parameters of all known large outer Galaxy molecular cloud complexes within $70° \leq l \leq 210°$ detected by this and previous CO surveys (Table 5) done with the GISS–Columbia telescope. Most of the longitude range studied here is well sampled only by surveys of 0°.5 angular resolution, which may have missed many clouds owing to effects of beam dilution and unfavorable sensitivity, but which should have revealed most large but not too distant (say, within 3 kpc) molecular cloud complexes. Surveys overlapped with our longitude range are also available at better angular resolution (e.g., Mead and Kutner 1986), but these are neither systematic nor well sampled and revealed no clouds more massive than 10^5 $M_\odot$. In the statistical study here, we will investigate the possible correlation between SNRs and *large* cloud complexes (but not the small ones distributed all over the Galactic disk).

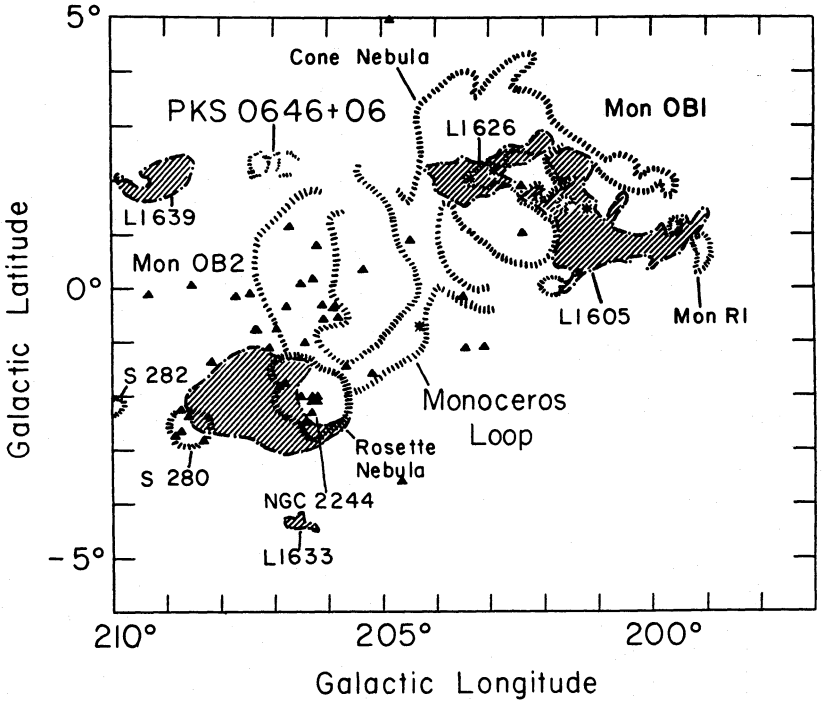

FIG. 19*a*

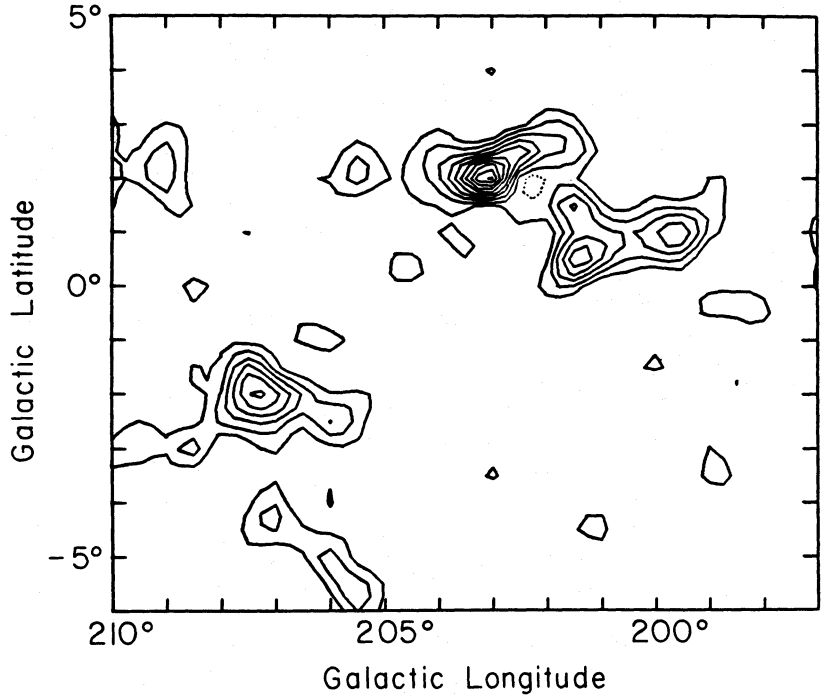

FIG. 19*b*

FIG. 19.—(*a*) Schematic map of young objects in Monoceros. The dark nebulae are denoted by shading, the optical emission by striated lines, and the most luminous stars of Mon OB1 by stars and of Mon OB2 by triangles (Turner 1976; Blitz 1978). (*b*) CO emission in Monoceros. Map integrated over velocity from -5 to 25 km s^{-1} with a contour interval of 3.5 K km s^{-1}.

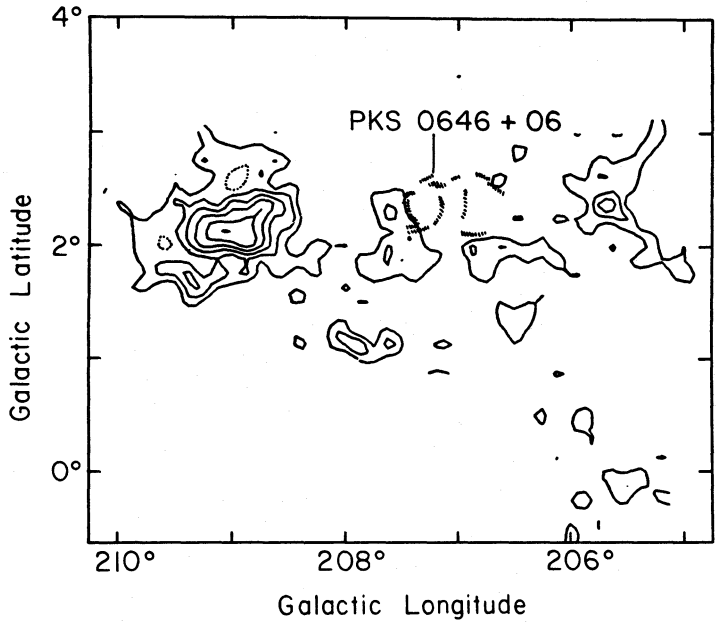

FIG. 20.—PKS 0646 + 06, map integrated over velocity from 0 to 25 km s^{-1} with a contour interval of 3 K km s^{-1}

TABLE 4

LARGE MOLECULAR CLOUD COMPLEXES IN THE OUTER GALAXY

(l, V)[a] (deg, km s^{-1})	CENTRAL POSITION l	CENTRAL POSITION b	RADIUS[b] (pc)	ADOPTED DISTANCE[c] (kpc)	MASS[d] ($10^5 M_\odot$)	ASSOCIATED OPTICAL OBJECT[e]	REFERENCE
(75, −57).....	74°.8	+1°.1	90	11.4	1.6	...	1
(77, −21).....	77.0	+0.1	90	7.2	1.8	...	2
(78, −32).....	77.6	+0.2	175	8.4	4.3	...	2
(78, −75).....	77.9	+0.7	145	12.7	5.8	...	2
(79, −62).....	78.5	+1.2	230	11.1	3.1	...	2
(79, −42).....	79.1	+1.1	235	8.9	8.7	DR 7	2
(80, −21).....	79.8	+0.8	120	6.5	3.3	...	2
(80, −32).....	80.2	+1.3	135	7.6	2.7	...	2
(85, −38).....	84.8	−0.4	130	7.2	8.5	...	1
(95, −44).....	94.6	−0.3	135	3.6	5.3	S 124	1
(95, −14).....	94.6	+0.3	115	2.8	2.0	...	1
(95, 0).....	94.7	+4.0	115	0.8	6.0	Cyg OB7	1
(110, −52).....	110.0	0.0	145	3.5	17.3	Cep OB1	1
(111, −38).....	111.3	−1.8	85	2.6	6.8	Cas OB2	1
(118, −3).....	118.3	+6.3	85	0.8	2.6	Cep OB4	1
(135, −40).....	135.4	+1.0	130	2.2	4.8	Cas OB6	1, 3
(160, −21).....	159.8	+2.9	120	5.6	5.4	S217	1
(167, −22).....	166.7	+3.5	85	5.0	1.3	...	1
(174, −18).....	174.0	+1.0	145	1.8[f]	5.7	S231/235	3
(183, −11).....	182.6	−0.8	60	2.1	1.5	S242	1
(191, 8).....	191.4	−0.1	145	1.5	11.0	Gem OB1	1
(202, 6).....	201.7	+1.5	45	0.8	1.1	Mon OB1	1
(205, 10).....	205.0	−13.0	50	0.5	1.3[g]	Ori OB1	4
(206, 15).....	206.4	−0.3	90	1.6	1.8	Mon OB2	1

[a] l is to the nearest degree of the cloud's center; V is the mean LSR radial velocity of CO emission line.
[b] Radius of the circle that just encloses most CO-emitting portions of each cloud or cloud complex.
[c] Kinematic distances from a flat rotation curve with $V_\odot = 250$ km s^{-1}, $R_\odot = 10$ kpc are adopted if no spectrophotometric distances are available for the associated optical objects.
[d] We assumed $N(H_2)/W_{CO} = 2.6 \times 10^{20}$ cm^{-2} K^{-1} km^{-1} s and a mean molecular weight of 2.72 for each H_2 molecule.
[e] Only the largest optical object is listed for each SNR.
[f] From Evans and Blair 1981.
[g] Only for the Ori B cloud.
REFERENCES.—(1) This work. (2) Huang *et al.* 1984. (3) Gottlieb *et al.* 1985. (4) Maddalena 1985.

TABLE 5

GISS–Columbia Large-Scale Outer Galaxy CO Surveys

Approximate Ranges of Survey					
l	b	V (km s^{-1})	Angular Resolution	rms Noise[a] (K)	Reference
(12°, 100°)	(−4°, 6°)	(−83, 83)[b]	60′	0.50	1
(60, 74)	(−1, 1)	(−104, 62)	8	0.35	2
(76, 81)	(−1, 3)	(−143, 23)	8	0.25	3
(84, 90)	(−1, 1)	(−104, 62)	8	0.35	2
(98, 180)	(−4, 10)	(−123, 43)	30	0.30	4
(105, 128)	(−4, 4)	(−123, 43)	8	0.65	5
(180, 210)	(−6, 5)	(−83, 83)	30	0.30	2

[a] In radiation temperature.

[b] Velocity coverage of from −113 to 53 km s^{-1} was used for $|b| < 3°$.

References.—(1) Dame and Thaddeus 1985. (2) Y.-L. Huang, unpublished. (3) Huang *et al.* 1984. (4) Gottlieb *et al.* 1985. (5) Cohen *et al.* 1980.

We identified a total of 24 large molecular cloud complexes, inferring the distances to 13 cloud complexes from the spectrophotometric distances of the accompanying OB associations or H II regions, while the distances to the 11 remaining cloud complexes, most of them distant clouds in the first quadrant, were estimated kinematically. We plotted the locations of the 26 SNRs in our sample and large cloud complexes on the projected plane of the sky (Fig. 21); objects of each kind are approximated by circles with diameters of their maximum angular sizes. Sixteen SNRs are found to lie within cloud complexes, five on the boundaries, and the remaining five outside the complexes.

A simple, two-dimensional statistical model was first used to estimate the probability $P_n(\geq k)$ that at least 16 ($= k$) positional coincidences between the 26 ($= n$) SNRs and the 24 large molecular cloud complexes are purely random. Assuming that each of the 26 SNRs is statistically independent and identical and each can either result in a coincidence or not, the probability $P_n(\geq k)$ is the cumulative binomial distribution

$$\sum_{j=k}^{n} \frac{n!}{j!(n-j)!} p^j (1-p)^{n-j} ,$$

where p is the probability that each SNR can result in a coincidence by chance. To calculate the value of p, the surface filling factor of large molecular cloud complexes on the projected plane of the sky, we have conservatively selected a range of 20° in Galactic latitude ($b = -5°$ to 15° for $l = 70°$–150° and $b = -10°$ to 10° for $l = 150°$–210°), because most SNRs and large cloud complexes in our study are just confined within this range (see Fig. 21). The calculated value of p is roughly 0.27; the corresponding probability $P_{26}(\geq 16)$ is 2.3×10^{-4}. Owing to exclusion of some undetected, distant clouds, this probability is underestimated, but because distant clouds generally span small solid angles it may not be significantly affected.

Although the small probability derived from the two-dimensional statistical model supports a causal relationship between SNRs and large molecular cloud complexes, a more realistic, three-dimensional model involving distances in the line of sight may be more convincing. In the three-dimensional model, we used two criteria to define a spatial coincidence between an SNR and a large molecular cloud complex:

1. The distances of the SNR and the cloud complex, within uncertainties, should agree.
2. The location of the SNR on the plane of the sky should lie within a circle that just encloses most CO-emitting portions of the cloud complex.

Table 6 presents 14 spatial coincidences between SNRs and large cloud complexes, including three SNRs that are accompanied by more than one cloud complex. To reduce bias in our selection of the sample, we confined the statistical study to the region within a heliocentric distance of 3 kpc; in previous surveys the beam dilution or low sensitivity may have limited detection of more distant clouds and SNRs. We further confined our study to a z-distance of ± 200 pc, because all the large molecular cloud complexes and most of the SNRs (except CTA 1 and the Crab Nebula) are concentrated in this range (Fig. 22). The locations of the large molecular cloud complexes in the Galactic plane compiled in Table 4 are presented in Figure 23. In the region selected, there are seven apparent spatial coincidences among the 11 SNRs and 11 large cloud complexes (Tables 4 and 6); of the 11 complexes, 10 have distances estimated from the spectrophotometric distances of the accompanying OB associations or H II regions, which are visible because nearby (≤ 3 kpc).

The probability of obtaining at least seven coincidences among 11 SNRs is $P_{11}(\geq 7)$, with p equal to the volume filling of large molecular cloud complexes. The value of p can be expressed as $V_c/V_{\rm tot}$, where $V_{\rm tot}$ is the total volume of the region selected and V_c the sum of all volumes of regions within which, for a coincidence to be claimed, a random SNR must be located. Each region is a cylinder that on the plane of the sky is a circle just enclosing most CO-emitting portions of the corresponding cloud complex and that on the line of sight includes every location in which an SNR could lie in order to be claimed as a coincidence with the cloud complex (see Appendix for details). Adopting a thickness τ of 400 pc perpendicular to

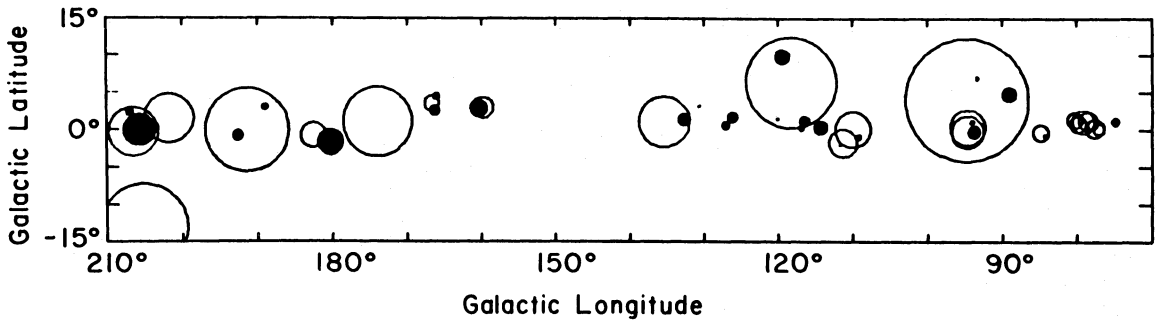

Fig. 21.—Distribution of SNRs and large molecular cloud. Each cloud is denoted by an open circle just enclosing most of the CO-emitting portions of the cloud; filled circles denote SNRs.

TABLE 6

APPARENT SPATIAL COINCIDENCES BETWEEN SUPERNOVA REMNANTS AND LARGE MOLECULAR CLOUDS

SNR	Distance[a] (kpc)	Note
G74.9+1.2	10.7	b
G84.2−0.8	6.3	b
G89.0+4.7	1.2	b
G93.3+6.9	5.7	c
G93.7−0.3	1.8	d
G94.0+1.0	4.7	d
G109.2−1.0	4.1	b
G111.7−2.1	3.0[e]	b
G114.3+0.3	3.0	c
G116.5+1.1	3.1	c
G116.9+0.2	4.5	c
G119.5+9.8	1.9	c
G120.1+1.4	2.3[e]	c
G126.2+1.6	3.6	c
G127.1+0.5	3.5	c
G130.7+3.1	2.2[e]	c
G132.7+1.3	1.6	b
G160.4+2.8	5.6[e]	b
G166.1+4.4	5.0[e]	b
G166.3+2.5	5.0[e]	b
G180.3−1.7	0.7[e]	c
G184.6−5.8	2.0[e]	c
G189.0+3.0	2.1	b
G192.8−1.1	2.6	b
G205.6−0.1	0.8	d
G206.9+2.3	4.3	c

[a] Heliocentric distances based on the Σ-D relation of Milne 1979, unless noted.

[b] Only one large cloud satisfies our criteria (see § IV) for a spatial coincidence between an SNR and a large molecular cloud.

[c] No accompanying large molecular cloud nearby.

[d] More than one large cloud satisfies our criteria for a spatial coincidence between an SNR and a large molecular cloud.

[e] Distances obtained by methods other than the Σ-D relation (see text).

the Galactic plane of the region selected, V_{tot} is calculated as 3.96 kpc^3. The probability p, with an estimate of 0.75 kpc^3 to V_c (see Appendix), is estimated to be 0.19; the corresponding probability $P_{11}(\geq 7)$ is approximately 1.4×10^{-3}.

Uncertainties in calculating $P_n(\geq k)$ in our three-dimensional model come mainly from the estimation of τ. The adopted value of 400 pc for τ, which is essentially the thickness of the cloud distribution, is probably underestimated, because presumably remnants of Type I SNs are distributed over a greater thickness than either remnants of Type II SNs or large molecular cloud complexes (both extreme Population I objects); our calculation of p should allow any type of SNR. Increasing τ from 400 to 550 pc order to include both CTA 1 and the Crab Nebula yields seven pairs among 13 SNRs; the corresponding probability $P_{13}(\geq 7)$, adopting a revised value of $p = 0.14$, becomes 8.3×10^{-4}, smaller than the previous estimate. Another potentially important uncertainty comes from our definition of the effective projected size of a cloud complex for a coincidence. Our definition of a circle enclosing most CO–emitting portions of the cloud complex is somewhat conservative, because many cloud complexes are elongated in shape. If other reasonable ways (e.g., choosing a region with a boundary at a certain distance beyond the complex's boundary) are used to define the effective size of a cloud complex, even though the estimation of p will be more complicated, the value of the probability $P_n(\geq k)$ should not differ much from our simplified case. The limit we set on heliocentric distance can also introduce uncertainty in calculating the probability $P_n(\geq k)$, but this uncertainty did not increase the probability significantly when we varied the distance limit (see Table 7).

TABLE 7

STATISTICS OF APPARENT COINCIDENCES BETWEEN SUPERNOVA REMNANTS AND LARGE MOLECULAR CLOUDS

r_0[a] (kpc)	ΣV_c (kpc^3)	V_{tot} (kpc^3)	p	n	k	$P_n(\geq k)$
3	0.75	3.96	0.19	11	7	1.4×10^{-3}
4	1.30	7.12	0.18	14	7	6.4×10^{-3}
5	1.66	11.32	0.15	20	11	3.9×10^{-5}

[a] Limit on heliocentric distance used for the statistical study (see § IV).

The small value of $P_n(\geq k)$ strongly argues for a causal relation in the apparent coincidences of most SNRs and the corresponding large molecular cloud complexes. However, it is worth mentioning that the small probability of $P_n(\geq k)$ cannot warrant an association between an individual SNR and its corresponding large cloud complex.

V. SUMMARY AND CONCLUSIONS

A well-sampled large-scale CO survey in and near every confirmed outer Galaxy SNR from $l = 70°$ to $210°$ was carried out to study the environment of SNRs. Within uncertainties of distance estimates, roughly half the SNRs surveyed are spatially coincident with large molecular cloud complexes. The probability that the apparent coincidences result from chance supernova explosions is estimated to be a few times 10^{-3} or less according to our two- or three-dimensional statistical

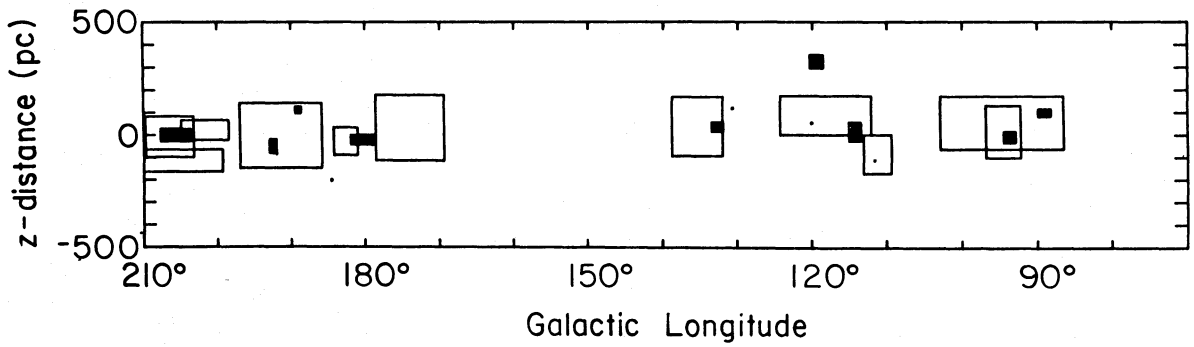

FIG. 22.—The z-distance vs. longitude maps for SNRs and large molecular clouds. Each object is denoted by a rectangle (open for clouds, filled for SNRs) which represents its range along either axis. When no other more reliable distance estimate to an SNR is available, the $|z|$-uncorrected Σ-D relation of Milne (1979) is used.

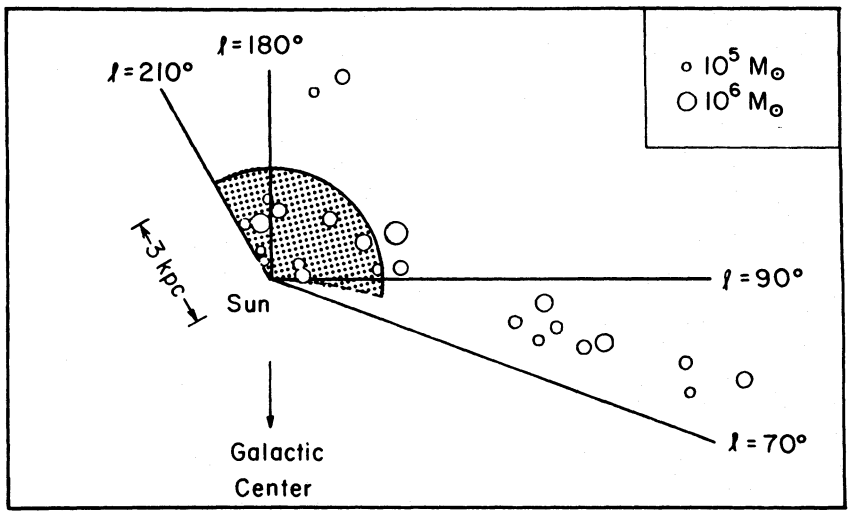

FIG. 23.—The locations of the large molecular clouds in the Galactic plane compiled in Table 4. The sizes of the circles are proportional to the cube roots of the cloud masses (a mass scale is given). The region selected for the statistical study in § IV is dotted.

model. This probability will not increase significantly if the assumptions used in the models are varied. It is, therefore, unlikely that this number of coincidences results from chance alone, although there is generally no direct evidence of an association between an SNR and a large molecular cloud complex.

The large molecular cloud complexes associated with SNRs in general show evidence of massive stars, either H II regions or OB associations. These SNRs are likely to result from Type II SNs, because in external galaxies only Type II SNs appear near H II regions or OB associations (Huang 1985). The progenitors of these SNRs may be the most massive member stars in the neighboring stellar associations presumably born in the large molecular cloud complexes. Although during their short lifetimes the progenitors migrated some distance from their birthplaces, they are still near the parent cloud complexes. A spatial coincidence between an SNR and a large molecular cloud complex therefore provides a potentially powerful means to classify the type (II, in this case) of SNRs in our Galaxy, which, owing to the lack of spectroscopic record, are usually impossible to classify. Our CO survey can also provide the large-scale molecular gas distribution near SNRs which can serve as basic information for further studies of the interaction between molecular clouds and SNRs through high-resolution CO and other observations.

We thank E. S. Palmer, S.-K. Pan, and T. M. Dame for help in operating and maintaining the GISS–Columbia telescope, S. van den Bergh for critical comments, and E. Sarot for editorial assistance.

APPENDIX

As stated in the text, the total effective volume (V_c) of large cloud complexes is defined as the sum of all volumes within regions where, for an apparent spatial coincidence between an SNR and a large cloud complex to be claimed, a random SNR must be located. Each region on the plane of the sky is approximated as a circle (Fig. 21) that just encloses most CO–emitting portions of the cloud complex. To take the uncertainties of estimating the distances into account, the region along the line of sight must start from a lower limit of heliocentric distance,

$$r_{cl} = [(1 - \mu_c)/(1 + \mu_{su})]r_c ,$$

to an upper limit,

$$r_{cu} = \min \{3 \text{ kpc}, [(1 + \mu_c)/(1 - \mu_{sl})]r_c\} ,$$

where μ_c is the uncertainty of the cloud complex's distance r_c, and μ_{su} and μ_{sl} are the upper and lower uncertainties of the SNR's distance respectively. In this case, the value of r_{cu} is confined to no more than 3 kpc, the limit of heliocentric distance set for our statistical study. The value of V_c can then be expressed as

$$V_c = \sum \pi(r_{cu} - r_{cl})a^2 ,$$

where a is the radius of the circle enclosing each cloud complex (Table 4) and the summation is over each known cloud complex in the region selected. Adopting $\mu_{sl} = 50\%$ and $\mu_{su} = 100\%$ (the uncertainty for Milne's Σ-D distance), the value of V_c in the region selected is calculated to be 0.75 kpc^3.

REFERENCES

Acker, A. 1978, *Astr. Ap. Suppl.*, **33**, 367.
Akhundova, G. V., Guseinov, O. Kh., and Rakhamimov, Sh. Yu. 1975, *Astrophysics*, **10**, 54.
Albinson, J. S., and Gull, S. F. 1982, in *Regions of Recent Star Formation*, ed. R. S. Roger and P. E. Dewdney (Dordrecht: Reidel), p. 193.
Allakhverdiyev, A. O., Amnuel, P. R., Guseinov, O. H., and Kasumov, F. K. 1983, *Ap. Space Sci.*, **97**, 261.
Allen, C. W. 1973, *Astrophysical Quantities* (3d ed.; London: Athlone).
Arsenault, R., and Roy, J.-R. 1984, *Pub. A.S.P.*, **96**, 496.
Bally, J., and Scoville, N. Z. 1980, *Ap. J.*, **239**, 121.
Black, J. H., and Raymond, J. C. 1984, *A.J.*, **89**, 411.
Blair, W. P., Kirshner, R. P., Gull, T. R., Sawyer, D. L., and Parker, R. A. R. 1980, *Ap. J.*, **242**, 592.
Blitz, L. 1978, Ph.D. thesis, Columbia University.
Blitz, L., Fich, M., and Stark, A. A. 1980, in *IAU Symposium 80, Interstellar Molecules*, ed. B. H. Andrew (Boston: Reidel), p. 213.
———. 1982, *Ap. J. Suppl.*, **49**, 183.
Bloemen, J. B. G. M., Caraveo, P. A., Hermsen, W., Lebrun, F., Maddalena, R. J., Strong, A. W., and Thaddeus, P. 1984, *Astr. Ap.*, **139**, 37.
Brandt, J. C., and Williamson, R. A. 1979, *Arcgaeoastronomy*, **1**, 1.
Braunsfurth, E. 1983, *Astr. Ap.*, **117**, 297.
Caswell, J. L. 1985, *A.J.*, **90**, 1076.
Caswell, J. L., and Lerche, I. 1979, *M.N.R.A.S.*, **187**, 201.
Chevalier, R. A. 1977, in *Supernovae*, ed. D. N. Schramm (Dordrecht: Reidel), p. 53.
Chevalier, R. A., Kirshner, R. P., and Raymond, J. C. 1980, *Ap. J.*, **235**, 186.
Chini, R., and Wink, J. E. 1984, *Astr. Ap.*, **139**, L5.
Clark, D. H., and Caswell, J. L. 1976, *M.N.R.A.S.*, **174**, 267.
Clemens, D. P. 1985, *Ap. J.*, **295**, 422.
Cohen, R. S., Cong, H., Dame, T. M., and Thaddeus, P. 1980, *Ap. J. (Letters)*, **239**, L53.
Cornett, R. H. 1977, Ph.D. thesis, University of Maryland.
Cornett, R. H., Chin, G., and Knapp, G. R. 1977, *Astr. Ap.*, **54**, 889.
Dame, T. M., Elmegreen, B. G., Cohen, R. S., and Thaddeus, P. 1986, *Ap. J.*, **305**, 892.
Dame, T. M., and Thaddeus, P. 1985, *Ap. J.*, **297**, 751.
Dickel, J. R., and DeNoyer, L. K. 1975, *A.J.*, **80**, 437.
Dickel, J. R., and Willis, A. G. 1980, *Astr. Ap.*, **85**, 55.
Doggett, J. B., and Branch, D. 1985, *A.J.*, **90**, 2303.
Dubout-Crillon, R. 1976, *Astr. Ap. Suppl.*, **25**, 25.
Duin, R. M., and Strom, R. G. 1975, *Astr. Ap.*, **39**, 33.
Dwarakanath, K. S., Shevgaonkar, R. K., and Sastry, Ch. V. 1982, *J. Ap. Astr.*, **3**, 207.
Erickson, W. C., and Mahoney, M. J. 1984, *Ap. J.*, **290**, 596.
Evans, N. J., II, and Blair, G. N. 1981, *Ap. J.*, **246**, 394.
Fesen, R. A., Blair, W. P., Kirshner, R. P., Gull, T. R., and Parker, R. A. R. 1981, *Ap. J.*, **247**, 148.
Fesen, R. A., and Kirshner, R. P. 1980, *Ap. J.*, **242**, 1023.
Fountain, W. F., Gary, G. A., and O'Dell, C. R. 1979, *Ap. J.*, **229**, 971.
Furst, E., Reich, W., and Steube, R. 1984, *Astr. Ap.*, **133**, 11.
Geldzahler, B. J., and Shaffer, D. B. 1982, *Ap. J. (Letters)*, **260**, L69.
Georgelin, Y. M. 1975, Thèse de doctorat, Université de Provence.
Georgelin, Y. M., Georgelin, Y. P., and Roux, S. 1973, *Astr. Ap.*, **25**, 337.
Goss, W. M., Mantovani, F., Salter, C. J., Tomasi, P., and Velusamy, T. 1984, *Astr. Ap.*, **138**, 469.
Gottlieb, E. W., Brock, J. E., and Thaddeus, P. 1985, unpublished.
Graham, D. A., Haslam, C. G. T., Salter, C. J., and Wilson, W. E. 1982, *Astr. Ap.*, **109**, 145.
Green, D. A. 1984, *M.N.R.A.S.*, **209**, 449.
Green, D. A., and Gull, S. F. 1982, *Nature*, **299**, 606.
Gregory, P. C., Braun, R., Fahlman, G. G., and Gull, S. F. 1983, in *IAU Symposium 101, Supernova Remnants and Their X-Ray Emission*, ed. J. Danziger and P. Gorenstein (Dordrecht: Reidel), p. 437.
Greisen, E. W. 1973, *Ap. J.*, **184**, 379.
Haslam, C. G. T., Pauls, T., and Salter, C. J. 1980, *Astr. Ap.*, **92**, 57.
Haslam, C. G. T., and Salter, C. J. 1971, *M.N.R.A.S.*, **151**, 385.
Hodge, P. W. 1983, *Pub. A.S.P.*, **95**, 721.
Huang, Y.-L. 1985, Ph.D. thesis, Columbia University.
Huang, Y.-L., Dame, T. M., Pan, S.-K., and Thaddeus, P. 1984, *Bull. AAS*, **16**, 727.
Huang, Y.-L., Dickman, R. L., and Snell, R. L. 1986, *Ap. J. (Letters)*, **302**, L63.
Huang, Y.-L., and Thaddeus, P. 1985, *Ap. J. (Letters)*, **295**, L13.
Hughes, M. P., Thompson, A. R., and Colvin, R. S. 1971, *Ap. J. Suppl.*, **23**, 323.
Hughes, V. A., Harten, R. H., Costain, C. H., Nelson, L. A., and Viner, M. R. 1984, *Ap. J.*, **283**, 147.
Humphreys, R. M. 1978, *Ap. J. Suppl.*, **38**, 309.
Kafatos, M., Sofia, S., Bruhweiler, F., and Gull, T. 1980, *Ap. J.*, **242**, 294.
Kazes, I., and Caswell, J. L. 1977, *Astr. Ap.*, **58**, 449.
Kirshner, R. P., and Arnold, C. N. 1979, *Ap. J.*, **229**, 147.
Knapp, G. R., Tremaine, S. D., and Gunn, J. E. 1978, *A.J.*, **83**, 1585.
Kundu, M. R., Angerhofer, P. E., Furst, E., and Hirth, W. 1980, *Astr. Ap.*, **92**, 225.
Lada, C. J., Elmegreen, B. G., Cong, H.-I., and Thaddeus, P. 1978, *Ap. J. (Letters)*, **226**, L39.
Lalitha, P., Mantovani, F., Salter, C. J., and Tomasi, P. 1984, *Astr. Ap.*, **131**, 196.
Landecker, T. L., Higgs, L. A., and Roger, R. S. 1984, *A.J.*, **90**, 1082.
Landecker, T. L., Pineault, S., Routledge, D., and Vaneldik, J. F. 1982*a*, *Ap. J. (Letters)*, **261**, L41.
Landecker, T. L., Roger, R. S., and Dewdney, P. E. 1982*b*, *A.J.*, **87**, 1379.
Lebrun, F., *et al.* 1983, *Ap. J.*, **274**, 231.
Lindoff, U. 1969, *Arkiv Astr.*, **5**, 221.
Lozinskaya, T. A. 1976, *Soviet Astr.*, **20**, 19.
———. 1981, *Soviet Astr. Letters*, **7**, 17.
Lozinskaya, T. A., and Sitnik, T. G. 1980, *Soviet Astr.*, **24**, 572.
MacConnell, D. J. 1968, *Ap. J. Suppl.*, **16**, 275.
Maddalena, R. J. 1985, Ph.D. thesis, Columbia University.
Mantovani, F., Nanni, M., Salter, C. J., and Tomasi, P. 1982, *Astr. Ap.*, **105**, 176.
Matthews, H. E., Baars, J. W. M., Wendker, H. J., and Goss, W. M. 1977, *Astr. Ap.*, **55**, 1.
Mayall, N. U., and Oort, J. H. 1942, *Pub. A.S.P.*, **54**, 95.
Maza, J., and van den Bergh, S. 1976, *Ap. J.*, **204**, 519.
Mead, K., and Kutner, M. 1986, private communication.
Milne, D. K. 1979, *Australian J. Phys.*, **32**, 83.
Minkowski, R. 1968, in *Stars and Stellar Systems*, Vol. **7**, *Nebulae and Interstellar Matter*, ed. B. M. Middlehurst (Chicago: University of Chicago Press), p. 623.
———. 1971, in *IAU Symposium 46, The Crab Nebula*, ed. R. D. Davies and F. G. Smith (Dordrecht: Reidel), p. 241.
Moffat, A. F. J., Fitzgerald, M. P., and Jackson, P. D. 1979, *Astr. Ap. Suppl.*, **38**, 197.
Montmerle, T. 1979, *Ap. J.*, **231**, 95.
Myers, P. C., Dame, T. M., Thaddeus, P., Cohen, R. S., Silverberg, R. F., Dwek, E., and Hauser, M. G. 1986, *Ap. J.*, **301**, 398.
Nomoto, K. 1983, in *IAU Symposium 101, Supernova Remnants and Their X-Ray Emission*, ed. J. Danziger and P. Gorenstein (Dordrecht: Reidel), p. 139.
Pan, S.-K., Feldman, M. J., Kerr, A. R., and Timbie, P. 1983, *Appl. Phys. Letters*, **43**, 786.
Parker, R. A. R., Gull, T. R., and Kirshner, R. P. 1979, NASA SP-434.
Pauls, T., van Gorkom, J. H., Goss, W. M., Shaver, P. A., Dickey, J. M., and Kulkarni, S. 1982, *Astr. Ap.*, **112**, 120.
Phillips, A. P., Gondhalekar, P. M., and Blades, J. C. 1981, *M.N.R.A.S.*, **195**, 485.
Pismis, P., and Hasse, I. 1980, *Rev. Mexicana Astr. Ap.*, **5**, 39.
Recillas-Cruz, E., and Pismis, P. 1979, *Rev. Mexicana Astr. Ap.*, **4**, 337.
Reich, W. 1983, *Naturwissenschaften*, **70**, 1.
Reich, W., and Braunsfurth, E. 1981, *Astr. Ap.*, **99**, 17.
Rickard, J. J. 1968, *Ap. J.*, **152**, 1019.
Roger, R. S., and Costain, C. H. 1976, *Astr. Ap.*, **51**, 151.
Sakhibov, F. Kh. 1980, *Soviet Astr. Letters*, **6**, 56.
Salter, C. J., Pauls, T., and Haslam, C. G. T. 1978, *Astr. Ap.*, **66**, 77.
Schmidt, M. 1965, in *Stars and Stellar Systems*, Vol. **5**, *Galactic Structure*, ed. A. Blaauw and M. Schmidt (Chicago: University of Chicago Press), p. 513.
Schwarz, U. J., Arnal, E. M., and Goss, W. M. 1980, *M.N.R.A.S.*, **192**, 67p.
Scoville, N. Z., Irvine, W. M., Wannier, P. G., and Predmore, C. R. 1977, *Ap. J.*, **216**, 320.
Sieber, W., Haslam, C. G. T., and Salter, C. J. 1979, *Astr. Ap.*, **74**, 361.
Sieber, W., Salter, C. J., and Mayer, C. J. 1981, *Astr. Ap.*, **103**, 393.
Sofue, Y., Furst, E., and Hirth, W. 1980, *Pub. Astr. Soc. Japan*, **32**, 1.
Spinrad, H., Stauffer, J., and Harlan, E. 1979, *Pub. A.S.P.*, **91**, 619.
Tammann, G. A. 1982, in *Supernovae: A Survey of Current Research*, ed. M. J. Rees and R. J. Stoneham (Dordrecht: Reidel), p. 371.
Trimble, V. 1973, *Pub. A.S.P.*, **85**, 579.
Turner, D. G. 1976, *Ap. J.*, **210**, 65.
van den Bergh, S. 1971, *Ap. J.*, **165**, 457.
———. 1978, *Ap. J. (Letters)*, **220**, L9.
———. 1983, in *IAU Symposium 101, Supernova Remnants and Their X-ray Emission*, ed. J. Danziger and P. Gorenstein (Dordrecht: Reidel), p. 597.
van den Bergh, S., Marscher, A. P., and Terzian, Y. 1973, *Ap. J. Suppl.*, **26**, 19.
Verschuur, G. L. 1973, *Astr. Ap.*, **27**, 73.
Vidal-Madjar, A., Laurent, C., Pettini, M., Paul, J. A., and Oliver, M. 1982, in *Proc. 3d European IUE Conf.*, ed. E. Rolfe, A, Heck, and B. Battrick (Noordwijk: European Space Agency, Scientific and Technical Publications Branch), p. 421.
Weiler, K. W., and Shaver, P. A. 1978, *Astr. Ap.*, **70**, 389.
Williams, D. R. W. 1973, *Astr. Ap.*, **28**, 309.
Willis, A. G. 1973, *Astr. Ap.*, **26**, 237.
Willis, A. G., and Dickel, J. R. 1971, *Ap. Letters*, **8**, 203.
Wilson, A. S., and Weiler, K. W. 1976, *Astr. Ap.*, **49**, 357.
Wootten, H. A. 1978, Ph.D. thesis, The University of Texas at Austin.
Wramdemark, S. 1981, *Astr. Ap. Suppl.*, **43**, 103.

Yi-Long Huang: Five College Radio Astronomy Observatory, 619 Lederle Graduate Research Center, University of Massachusetts, Amherst, MA 01003

Patrick Thaddeus: Harvard-Smithsonian Center for Astrophysics, 60 Garden Street, Cambridge, MA 02138